

Hierarchical Bayes Approach to Personalized Federated Unsupervised Learning

Kaan Ozkara
University of California, Los Angeles
kaan@ucla.edu

Bruce Huang
University of California, Los Angeles
brucehuang@ucla.edu

Ruida Zhou
University of California, Los Angeles
ruida@ucla.edu

Suhas Diggavi
University of California, Los Angeles
suhas@ee.ucla.edu

Abstract

Statistical heterogeneity of clients' local data is an important characteristic in federated learning, motivating personalized algorithms tailored to the local data statistics. Though there has been a plethora of algorithms proposed for personalized supervised learning, discovering the structure of local data through personalized unsupervised learning is less explored. We initiate a systematic study of such personalized unsupervised learning by developing algorithms based on optimization criteria inspired by a hierarchical Bayesian statistical framework. We develop adaptive algorithms that discover the balance between using limited local data and collaborative information. We do this in the context of two unsupervised learning tasks: personalized dimensionality reduction and personalized diffusion models. We develop convergence analyses for our adaptive algorithms which illustrate the dependence on problem parameters (*e.g.*, heterogeneity, local sample size). We also develop a theoretical framework for personalized diffusion models, which shows the benefits of collaboration even under heterogeneity. We finally evaluate our proposed algorithms using synthetic and real data, demonstrating the effective sample amplification for personalized tasks, induced through collaboration, despite data heterogeneity.

1 Introduction

One of the goals of unsupervised learning is to discover the underlying structure in data and use this for tasks such as dimensionality reduction and generating new samples from the data distribution. We might want to perform this task on local data of a client, *e.g.*, data collected from personal sensors or other devices; such data could have heterogeneous statistics across clients. The desired *personalized* task should be tailored to the particular distribution of the local data, and hence to discover this structure one might need a significant amount of local data. There might be insufficient local samples for the task, motivating collaboration between clients. Moreover, as argued in the federated learning (FL) paradigm, we would like to leverage data across clients without explicit data sharing [26, 16]. In this paper, we initiate a systematic study of personalized federated unsupervised learning, where clients collaborate to discover personalized structure in their (heterogeneous) local data.

There has been a plethora of personalized learning models proposed in the literature, mostly for *supervised* federated learning [11, 8, 24, 30, 28]. These methods were motivated by the statistical heterogeneity of local data, causing a single “global” model to perform poorly on local data. The different personalized federated supervised learning algorithms were unified in [28] using an empirical/hierarchical Bayes statistical model [10], which also suggested new *supervised* learning algorithms. However, there has been much less work on personalized federated unsupervised learning. We will build on the statistical approach studied in [28] for supervised learning, applying it to personalized unsupervised learning. This leads to new federated

algorithms for personalized dimensionality reduction and personalized diffusion-based generative models for heterogeneous data.

A question is how to use local data and learn from others despite heterogeneity. The hierarchical Bayes framework [10] suggests using an estimated population distribution effectively as a prior. However, the challenge is to efficiently estimate it, enabling each client to combine local data and collaborative information for the unsupervised learning task. We do this by *simultaneously* learning a global model (a proxy for the population model) and learning a local model by adaptively estimating its discrepancy to balance the global and local information. In Section 2, we define this through a loss function, making it amenable to a standard distributed gradient descent approach. Our main contributions are as follows.

Unsupervised collaboration learning criteria: Section 2 develops and uses the hierarchical Bayes framework for personalized dimensionality reduction and personalized (generative) diffusion models. We develop an *Adaptive Distributed Empirical-Bayes based Personalized Training* (ADEPT) criterion which embeds the balance between local data and collaboration for these tasks (see below). As far as we are aware, these are the first explicit criteria for such personalized federated unsupervised learning tasks.

Personalized dimensionality reduction: Section 3 develops adaptive personalized algorithms for linear (PCA) (ADEPT-PCA) and non-linear (auto-encoders) (ADEPT-AE) for dimensionality reduction. We also demonstrate its convergence in Theorems 3.3 and 3.12. In Remark 3.13, we see that these allow us to theoretically examine the impact of heterogeneity, number of local samples and number of clients, on optimization performance. We believe that these are the first adaptive algorithms for personalized dimensionality reduction and their convergence analyses. Finally in Section 5¹, we evaluate ADEPT-PCA and ADEPT-AE on synthetic and real data showing the benefits of adaptive collaboration. For example, Table 2 shows effective amplification of as much as 20× in local sample complexity through collaboration.

Personalized diffusion models: Section 4 develops an adaptive personalized diffusion generative model (ADEPT-DGM) to generate novel samples for local data statistics. We believe that ADEPT-DGM is the first algorithm for federated personalized diffusion. We develop a theory for such personalized federated diffusion models through our statistical framework, and use this to demonstrate, in Theorem 4.5, conditions when collaboration can improve performance, despite statistical heterogeneity. Finally in Section 5, we evaluate ADEPT-DGM, demonstrating the value of adaptive collaboration despite heterogeneity, as well as significant performance benefits for “worst” clients.

Related work: As mentioned earlier, there have been several recent works on personalized *supervised* learning (see next paragraph). There has been much less attention given to personalized federated unsupervised learning. The closest work to ours on personalized dimensionality reduction is [35, 29] which study personalized PCA algorithms. [35] has a restrictive assumption that principal components for global and local models are non-overlapping. [29] uses the hierarchical Bayes statistical model to develop a criterion for personalized PCA; however, the authors assume heterogeneity of the setting is known; in contrast, ADEPT-PCA learns and adapts the solution accordingly. There is some literature on specific tasks such as training recommender systems [21, 32], grouping clients based on latent representations [44], generating data to improve performance of personalized supervised learning [3, 31]. However, our approach to developing personalized dimensionality reduction for heterogeneous data is distinct from them. We are not aware of any FL work for personalized diffusion generative models. There is work using pre-trained diffusion models and then fine-tuning them [34, 46, 27, 23]. However, these do not fit into the federated learning paradigm, and require data collection from clients to obtain the pre-trained model. One way to view our approach is to *simultaneously* build such “global” models (akin to pre-trained models) and individual (personalized) models, while not sharing data. Beyond these above works, some more related works are as follows: Personalized Federated Learning (FL) has seen recent advances with diverse approaches for learning personalized models. These approaches encompass meta-learning-based methods [11, 1, 17], regularization techniques [7, 24, 13], clustered FL [47, 24, 12, 25], knowledge distillation strategies [22, 30], multi-task learning [8, 36, 43, 45], and the utilization of common representations [9, 40, 6]. Additionally, recently there have been works on using a hierarchical Bayesian view to derive novel personalized supervised FL algorithms [28, 4, 20]. Adaptation is also considered in [28, 4]. In [4], variance estimation is performed for supervised learning to estimate the heterogeneity within the local models and the estimated variance is used to form an initialization for each local model to be trained on. However, if we apply variance estimation to our criterion, we observe an early stopping issue during the training. In

¹Our code is available at <https://github.com/kazkara/adept>.

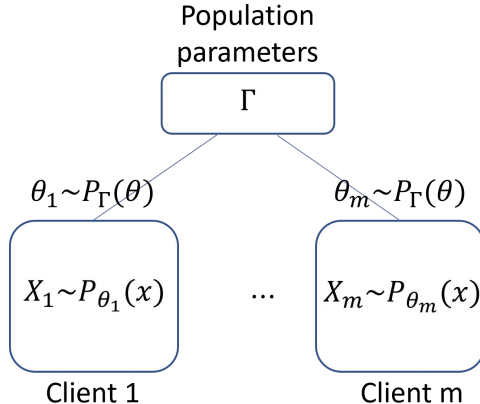


Figure 1: Hierarchical Bayesian model of data distribution

contrast, ours is based on a standard gradient descent. Moreover, they do not examine convergence which we do in our unsupervised algorithms. In [28], the authors consider an adaptation for supervised learning based on the KL-divergence criterion and do not have hyper prior. Moreover, a convergence analysis is not explored in their algorithm. In that case, the σ is inclined to smaller values or even vanishes during the training, and our ADEPT criterion resolves the issue by introducing the hyper prior. [42] investigated local features of globally trained diffusion models through FedAvg, but they do not consider personalized generation.

2 Problem Formulation

We present a hierarchical Bayesian framework for the personalized unsupervised learning, using it to develop optimization criteria for federated personalized dimensionality reduction and personalized diffusion models. First we state some preliminaries for notation. For the notations used in this paper:

- We use bold lowercase letters (such as \mathbf{u} , \mathbf{v}) to denote vectors and we use bold uppercase letters (such as \mathbf{U} , \mathbf{V}) to denote matrices.
- Given a composite function $f(\mathbf{u}, \mathbf{v})$, we denote $\nabla f(\mathbf{u}, \mathbf{v})$ or $\nabla_{(\mathbf{u}, \mathbf{v})} f(\mathbf{u}, \mathbf{v})$ as the gradient; $\nabla_{\mathbf{u}} f(\mathbf{u}, \mathbf{v})$ and $\nabla_{\mathbf{v}} f(\mathbf{u}, \mathbf{v})$ as the partial gradients with respect to \mathbf{u} and \mathbf{v} .
- For a vector \mathbf{u} , $\|\mathbf{u}\|$ denotes the ℓ_2 -norm $\|\mathbf{u}\|_2$. For a matrix \mathbf{U} , $\|\mathbf{U}\|_2$ and $\|\mathbf{U}\|_{op}$ both denote the ℓ_2 -norm (operator norm) of the matrix and $\|\mathbf{U}\|$, $\|\mathbf{U}\|_F$ denotes the Frobenius norm of the matrix.
- We use $\{\mathbf{U}_i\}_{i=1}^m$ or $\{\mathbf{U}_i\}$ (when the context is clear) to denote the collection $\{U_1, \dots, U_m\}$. When there are multiple indices, we use $\{\mathbf{U}_{i,t}\}_i := \{U_{1,t}, \dots, U_{m,t}\}$ to denote the collection over index i .

2.1 Hierarchical Bayes for personalized learning

The *statistical model* based on hierarchical Bayes, suitable for federated unsupervised learning, is illustrated in Figure 1. There are m clients. Each client i is associated with a parameter θ_i and has a local dataset \mathbf{X}_i consisting of n data points $(\mathbf{x}_{i1}, \dots, \mathbf{x}_{in})$ i.i.d. from distribution $p(\mathbf{x}|\theta_i)$. The parameters obey a population distribution (a.k.a. prior distribution in the Bayesian model) $p(\theta|\Gamma)$ parameterized by Γ . We have a (carefully designed) hyper prior distribution π over Γ , i.e., $\Gamma \sim \pi$ to prevent ill-posedness. This statistical model defines the joint distribution

$$p_{\Gamma, \{\theta_i\}, \{\mathbf{X}_i\}}(\Gamma, \theta_1, \dots, \theta_m, \mathbf{X}_1, \dots, \mathbf{X}_m) = \pi(\Gamma) \prod_{i=1}^m p(\theta_i|\Gamma) \prod_{i=1}^m \prod_{j=1}^n p(\mathbf{x}_{ij}|\theta_i). \quad (1)$$

We learn the distribution parameters $\Gamma, \{\boldsymbol{\theta}_i\}$ from data $\{\mathbf{X}_i\}$ by maximizing the joint distribution (a.k.a. maximum a posteriori), by minimizing the ADEPT loss function:

$$f(\{\boldsymbol{\theta}_i\}, \Gamma; \{\mathbf{X}_i\}) = \frac{1}{m} \sum_{i=1}^m f_i(\boldsymbol{\theta}_i; \mathbf{X}_i) + R(\{\boldsymbol{\theta}_i\}, \Gamma),$$

where $f_i(\boldsymbol{\theta}_i; \mathbf{X}_i) := -\sum_{j=1}^n \log(p(\mathbf{x}_{ij}|\boldsymbol{\theta}_i))$ is the local loss function for client i reflecting the likelihood of the local dataset, and $R(\{\boldsymbol{\theta}_i\}, \Gamma) = -\frac{1}{m} \log \pi(\Gamma) - \frac{1}{m} \sum_{i=1}^m \log p(\boldsymbol{\theta}_i|\Gamma)$ is a regularization allowing the collaboration among clients. When the likelihood function is not easy to optimize, we leverage surrogates such as evidence lower bound (ELBO) instead.

In this work, we focus on a Gaussian population distribution over an d_θ -dimensional normed metric space $(\Theta, \|\cdot\|)^2$. Specifically, $\Gamma = (\boldsymbol{\mu}, \sigma)$, the parameters $\boldsymbol{\theta}, \boldsymbol{\mu} \in \Theta$ and $p(\boldsymbol{\theta}|\Gamma) = \frac{1}{(2\pi\sigma^2)^{d_\theta/2}} \exp(-\frac{\|\boldsymbol{\theta}-\boldsymbol{\mu}\|^2}{2\sigma^2})$, where d is the dimensionality of $\boldsymbol{\theta}$ and $\boldsymbol{\mu}$ has the same dimension as $\boldsymbol{\theta}$. We assume an improper (non-informative) hyper prior π over $\Gamma = (\boldsymbol{\mu}, \sigma)$, as $\boldsymbol{\mu} \sim \mathcal{N}(0, \infty \cdot \mathbf{I}_{d_\theta})$ and σ^2 follows an inverse gamma distribution parameterized by a hyper-parameter ξ , i.e., $\pi(\boldsymbol{\mu}, \sigma) \propto \exp(\frac{m\xi}{\sigma^2})$ ³. We thus have the regularization

$$R(\{\boldsymbol{\theta}_i\}, \Gamma) = -\frac{1}{m} \log \pi(\Gamma) - \frac{1}{m} \sum_{i=1}^m \log p(\boldsymbol{\theta}_i|\Gamma) = \frac{1}{m} \sum_{i=1}^m \frac{2\xi + \|\boldsymbol{\mu} - \boldsymbol{\theta}_i\|^2}{2\sigma^2} + d_\theta \log \sigma. \quad (2)$$

2.2 Personalized Dimensionality Reduction

Linear Dimensionality Reduction: The linear dimensionality reduction is equivalent to PCA. We extend a personalized PCA formulation that was previously studied in [29] by introducing adaptivity i.e. optimizing the loss over σ . In this setting, the dataset from client i is $\mathbf{X}_i \in \mathbb{R}^{d \times n}$ containing n samples of d dimensional vectors. Let us denote $\mathbf{S}_i = \frac{1}{n} \mathbf{X}_i \mathbf{X}_i^\top$ as the sample covariance matrix of client i . For notational consistency with canonical PCA notation, we set the parameters $\boldsymbol{\theta}_i = \mathbf{U}_i \in \mathbb{R}^{d \times r}$. Similar to [29], we adopt the probabilistic view of PCA [41],

$$\mathbf{x}_{ij} = \mathbf{U}_i \mathbf{z}_{ij} + \boldsymbol{\epsilon}_{ij}, \quad (3)$$

where $\mathbf{z}_{i1}, \dots, \mathbf{z}_{in} \stackrel{i.i.d.}{\sim} \mathcal{N}(\mathbf{0}, \mathbf{I}_r)$ and $\boldsymbol{\epsilon}_{i1}, \dots, \boldsymbol{\epsilon}_{in} \stackrel{i.i.d.}{\sim} \mathcal{N}(\mathbf{0}, \sigma_\epsilon^2 \mathbf{I}_d)$. This results in the likelihood function $p(\mathbf{X}_i|\boldsymbol{\theta} = \mathbf{U}_i) = \mathcal{N}(\mathbf{0}, \mathbf{U}_i \mathbf{U}_i^\top + \sigma_\epsilon^2 \mathbf{I})$. Recall that the prior parameter is $\Gamma = (\boldsymbol{\mu}, \sigma)$, here for notational consistency we use $\mathbf{V} = \boldsymbol{\mu}$. The underlying metric space $(\Theta, \|\cdot\|)$ containing the parameters \mathbf{U} and \mathbf{V} in the Steifel manifold where $St(d, r) := \{\mathbf{U} \in \mathbb{R}^{d \times r} | \mathbf{U}^\top \mathbf{U} = \mathbf{I}\}$. The metric is $d(\mathbf{V}, \mathbf{U}) = \|P_{\mathcal{T}_{\mathbf{V}}}(\mathbf{U})\|$ where $P_{\mathcal{T}_{\mathbf{V}}}(\mathbf{U}) = \mathbf{U} - \frac{1}{2} \mathbf{V}(\mathbf{V}^\top \mathbf{U} + \mathbf{U}^\top \mathbf{V})$ is the projection of \mathbf{U} onto the tangent space at \mathbf{V} . Because computing the (geodesic) distance on $St(d, r)$ is hard, the defined metric first projects a matrix to the tangent space of another matrix and then computes the Frobenius norm. The personalized unsupervised learning is then minimizing the ADEPT-PCA loss function:

$$\min_{\{\mathbf{U}_i\}, \mathbf{V}, \sigma} f^{\text{pca}}(\{\mathbf{U}_i\}, \mathbf{V}, \sigma; \{\mathbf{X}_i\}) := \frac{1}{m} \left(\sum_{i=1}^m \frac{n}{2} (\log(|\mathbf{W}_i|) + \text{tr}(\mathbf{W}_i^{-1} \mathbf{S}_i)) + \frac{2\xi + d^2(\mathbf{V}, \mathbf{U}_i)}{2\sigma^2} \right) + d_\theta \log \sigma \quad (4)$$

s.t. $\mathbf{V}^\top \mathbf{V} = \mathbf{I}, \mathbf{U}_i^\top \mathbf{U}_i = \mathbf{I} \quad \forall i \in [m]$; where $\mathbf{W}_i = (\mathbf{U}_i \mathbf{U}_i^\top + \sigma_\epsilon^2 \mathbf{I})$.

Non-linear dimensionality reduction: While PCA is a good starting point for dimensionality reduction, it cannot capture non-linear relations between the latent variable and the observed space. Hence, one can extend (3) to model non-linearity as follows,

$$\mathbf{x}_{ij} = \psi_{\boldsymbol{\theta}_i^d}(\mathbf{z}_{ij}) + \boldsymbol{\epsilon}_{ij}, \quad (5)$$

²Note that this general framework can be applied to any general (parametric) population distribution.

³Inverse-Gamma distribution is conjugate prior distribution for the variance term.

where θ_i^d parameterizes a non-linear decoding map from the latent space to the observed space. We can parameterize the encoder structure such that $\mathbf{z}_{ij} = g_{\theta_i^e}(X_{ij})$. Using Gaussian distribution we get the ADEPT-AE criterion:

$$\arg \min_{\{\theta_i\}, \mu, \sigma} f^{ae}(\{\theta_i\}, \mu, \sigma) = \frac{1}{m} \sum_{i=1}^m \left(\|\mathbf{X}_i - \psi_{\theta_i^d}(g_{\theta_i^e}(\mathbf{X}_i))\|_F^2 + \frac{2\xi + \|\mu - \theta_i\|^2}{2\sigma^2} \right) + d_\theta \log \sigma \quad (6)$$

where μ is the global model and $\{\theta_i\}$ are the autoencoders of the clients and viewed as the concatenation of θ_i^e and θ_i^d .

2.3 Personalized Generation through Diffusion Models

The denoising diffusion model has attracted attention recently due to its capability of generating high-quality images and the theoretical foundation of the stochastic differential equations [33, 37]. The mathematical model of a diffusion model is the following stochastic differential equation [39]

$$d\mathbf{x}_t = d\mathbf{w}_t \quad (\text{variance exploding process}), \quad (7)$$

where \mathbf{w}_t is a standard d -dimensional Brownian motion. For time $t \in [0, T]$, its time-reversed process is

$$d\mathbf{x}_t^\leftarrow = \nabla \ln p_{\mathbf{x}_{T-t}}(\mathbf{x}_t^\leftarrow) dt + d\mathbf{w}_t^\leftarrow, \quad (8)$$

where $p_{\mathbf{x}_t}$ is the probability density function of \mathbf{x}_t , \mathbf{w}_t^\leftarrow is a standard Wiener process. It can be verified that X_t^\leftarrow follows the same distribution as \mathbf{x}_{T-t} . More strongly, suppose X_0^\leftarrow has the same distribution as \mathbf{x}_T , and then the two processes $\{\mathbf{x}_{T-t}\}_{t \in [0, T]}$ and $\{\mathbf{x}_t^\leftarrow\}_{t \in [0, T]}$ have the same distribution.

Suppose that the score function $\nabla \ln p_{\mathbf{x}_t}(\mathbf{x})$ can be represented by a neural network $\phi(\mathbf{x}; \theta, t) \in \mathbb{R}^d$ for some parameter θ . The data generation is then integration over the time-revised process (8) with the drift function $\phi(\mathbf{x}; \theta, t)$ and the starting distribution $\mathbf{x}_0^\leftarrow \sim \mathcal{N}(\mathbf{0}, \sigma_0^2 \mathbf{I}_d)$. The generated distribution $p(\mathbf{x}|\theta)$ is then implicitly defined without a closed form. [18, Eq (4)] shows that

$$\ln p(\mathbf{x}|\theta) \geq ELBO_\theta(\mathbf{x}) = -\frac{1}{2} \int_{t=0}^T \mathbb{E} \|\phi(\mathbf{x}_t; \theta, t) - \nabla_{\mathbf{x}_t} \ln p_{\mathbf{x}_t|\mathbf{x}_0}(\mathbf{x}_t|\mathbf{x})\|^2 dt + C \quad (9)$$

where $\mathbf{x}_t \sim \mathcal{N}(\mathbf{x}, \mathbf{I}_d)$ and C is some constant factor independent of θ . Accordingly, we use ELBO⁴ as a surrogate function for the negative log-likelihood; thus, the personalized loss function is $f_i(\theta_i; \mathbf{X}_i) = -ELBO_{\theta_i}(\mathbf{X}_i) = -\sum_{j=1}^n ELBO_{\theta_i}(\mathbf{x}_{ij})$. The personalized data generation is then minimizing the ADEPT-DGM loss function

$$\min_{\{\theta_i\}, \mu, \sigma^2} f^{\text{df}}(\{\theta_i\}, \mu, \sigma; \{\mathbf{X}_i\}) := \frac{1}{m} \sum_{i=1}^m \left(-ELBO_{\theta_i}(\mathbf{X}_i) + \frac{2\xi + \|\mu - \theta_i\|^2}{2\sigma^2} \right) + d_\theta \log \sigma. \quad (10)$$

3 Personalized Federated Dimensionality Reduction

In this section, we discuss our algorithms and convergence results on personalized adaptive dimensionality reduction.

3.1 Personalized Adaptive PCA: ADEPT-PCA

We introduce ADEPT-PCA (Algorithm 1) to train adaptive personalized PCA. On **line 7** we update the adaptivity parameter $\sigma_{i,t}$, on **lines 8, 10** we compute the projected gradients for personalized and global parameters. On **lines 9, 16** we update the personalized and global parameters through projected gradient descent and retraction. In Algorithm 1, we use the polar retraction to map the updated \mathbf{V} and \mathbf{U}_i back to the Steifel manifold. We define the polar retraction in the next section in detail.

To show the convergence of the algorithm we need the following standard assumption and naturally occurring lower bound on σ .

⁴Unlike the discrete case, for the continuous case, there are several definitions used for ELBO e.g. in [38, 19]; [18] uses the simplified definition in (9) to unify different ELBO definitions.

Algorithm 1 ADEPT-PCA Algorithm

Input: Number of iterations T and learning rates (η_1, η_2, η_3) .

- 1: **Initialize** local PCs $\{\mathbf{U}_{i,0}\}_{i=1}^m$, global PC \mathbf{V}_0 , and σ_0 .
- 2: Broadcast \mathbf{V}_0, σ_0 to the clients
- 3: **for** $t = 1$ **to** T **do**
- 4: **On the clients:**
- 5: **for** $i = 1$ **to** m : **do**
- 6: Receive $\mathbf{V}_{t-1}, \sigma_{t-1}$
- 7: $\sigma_{i,t} = \sigma_{t-1} - \eta_3 \frac{\partial}{\partial \sigma_{t-1}} f_i^{\text{pca}}(\mathbf{U}_{i,t-1}, \mathbf{V}_{t-1}, \sigma_{t-1})$
- 8: $\mathbf{g}_{i,t}^U = P_{\mathcal{T}_{\mathbf{U}_{i,t-1}}}(\nabla_{\mathbf{U}_{i,t-1}} f_i^{\text{pca}}(\mathbf{U}_{i,t-1}, \mathbf{V}_{t-1}, \sigma_{t-1}))$
- 9: $\mathbf{U}_{i,t} \leftarrow \mathcal{R}_{\mathbf{U}_{i,t-1}}(-\eta_1 \mathbf{g}_{i,t}^U)$
- 10: $\mathbf{g}_{i,t}^V = P_{\mathcal{T}_{\mathbf{V}_{t-1}}}(\nabla_{\mathbf{V}_{t-1}} f_i^{\text{pca}}(\mathbf{U}_{i,t}, \mathbf{V}_{t-1}, \sigma_{t-1}))$
- 11: $\mathbf{V}_{i,t} \leftarrow \mathbf{V}_{t-1} - \eta_2 \mathbf{g}_{i,t}^V$
- 12: Send $\mathbf{V}_{i,t}, \sigma_{i,t}$ to the server
- 13: **end for**
- 14: **At the server:**
- 15: Receive $\{\mathbf{V}_{i,t}\}_{i=1}^m$ and $\{\sigma_{i,t}\}_{i=1}^m$
- 16: $\mathbf{V}_t = \mathcal{R}_{\mathbf{V}_{t-1}}(\frac{1}{m} \sum_{i=1}^m \mathbf{V}_{i,t} - \mathbf{V}_{t-1})$
- 17: $\sigma_t = \frac{1}{m} \sum_{i=1}^m \sigma_{i,t}$
- 18: Broadcast \mathbf{V}_t, σ_t to the clients
- 19: **end for**

Output: Personalized PCs $\{\mathbf{U}_{1,T}, \dots, \mathbf{U}_{m,T}\}$.

Assumption 3.1. For each client i , the operator and Frobenius norms of \mathbf{S}_i are bounded by

$$\|\mathbf{S}_i\|_F \leq G_{i,F} \quad \text{and} \quad \|\mathbf{S}_i\|_{op} \leq G_{i,op},$$

and $G_{max,F} := \max_{i \in [m]} G_{i,F}, G_{max,op} := \max_{i \in [m]} G_{i,op}$. The assumption implies the Lipschitz smoothness properties of the loss function w.r.t. personalized PCs $\{\mathbf{U}_i\}$.

Lemma 3.2 (A lower bound on σ_t). *Given any $\omega \in (0, 1)$. Let the learning rate $\eta_3 \leq (1 - \omega) \frac{2\xi}{d_\theta}$ and the initialization $\sigma_0 \geq \omega \sqrt{\frac{2\xi}{d_\theta}}$. Then, for all $t \in [T]$, we have $\sigma_t \geq \omega \sqrt{\frac{2\xi}{d_\theta}}$.*

See Appendix A.1.1 for the proof. We will fix some $\omega \in (0, 1)$ for the rest of the paper and initialize σ_0 accordingly so that we can utilize the lower bound in Lemma 3.2. The bound is due to ξ to guarantee that the loss does not explode due to vanishing σ . Let us now define $\mathbf{g}_{i,t}^U = P_{\mathcal{T}_{\mathbf{U}_{i,t-1}}}(\nabla_{\mathbf{U}_{i,t-1}} f_i^{\text{pca}}(\mathbf{U}_{i,t-1}, \mathbf{V}_{t-1}, \sigma_{t-1}))$, $\mathbf{g}_t^V = \frac{1}{m} \sum_{i=1}^m P_{\mathcal{T}_{\mathbf{V}_{t-1}}}(\nabla_{\mathbf{V}_{t-1}} f_i^{\text{pca}}(\mathbf{U}_{i,t}, \mathbf{V}_{t-1}, \sigma_{t-1}))$, and $g_t^\sigma = \frac{\partial}{\partial \sigma_{t-1}} f^{\text{pca}}(\{\mathbf{U}_{i,t-1}\}_i, \mathbf{V}_{t-1}, \sigma_{t-1})$. Then, Algorithm 1 has the following convergence upper bound for finding a first-order stationary point.

Theorem 3.3 (Convergence of ADEPT-PCA Algorithm 1). *Let $G_t = \left(\frac{1}{m} \sum_{i=1}^m \|\mathbf{g}_{i,t}^U\|^2\right) + \|\mathbf{g}_t^V\|^2 + (g_t^\sigma)^2$. By choosing $\eta_1 = \min\{\frac{1}{3C_{\eta_1}}, 1\}$, $\eta_2 = \min\{\frac{1}{3C_{\eta_2}}, 1\}$, and $\eta_3 = \min\left\{\frac{\eta_1}{3(L_U^{(\sigma)})^2}, \frac{\eta_2}{3(L_V^{(\sigma)})^2}, \frac{1}{L_\sigma}\right\}$, we have*

$$\frac{1}{T} \sum_{t=1}^T G_t \leq \frac{3\Delta_T^{\text{pca}}}{T \min\{\eta_1, \eta_2, \eta_3\}},$$

where T is number of total iterations, $\Delta_T^{\text{pca}} = f^{\text{pca}}(\{\mathbf{U}_{i,0}\}_i, \mathbf{V}_0, \sigma_0) - f^{\text{pca}}(\{\mathbf{U}_{i,T}\}_i, \mathbf{V}_T, \sigma_T)$, and η_1, η_2, η_3 are the learning rates for updating \mathbf{U}_i , \mathbf{V} , and σ respectively. The constants are defined such that $f^{\text{pca}}(\cdot)$ is L_σ -smooth w.r.t. σ and $\mathbf{g}_{i,t}^U, \mathbf{g}_t^V$ are $L_U^{(\sigma)}, L_V^{(\sigma)}$ continuous w.r.t. σ respectively. C_{η_1}, C_{η_2} are defined in detail in the next section and depend on smoothness w.r.t. \mathbf{U}, \mathbf{V} .

We provide a detailed comment on the factors impacting the convergence rate in Remark 3.13.

3.1.1 Proof Outline for Theorem 3.3

For any point $\mathbf{U} \in St(d, r)$, a retraction at a point $\mathbf{U} \in St(d, r)$ is a map $\mathcal{R}_{\mathbf{U}} : \mathcal{T}_{\mathbf{U}} \rightarrow St(d, r)$ that induces local coordinates on the Stiefel manifold. In this work, we use polar retraction that is defined as $\mathcal{R}_{\mathbf{U}}(\mathbf{V}) = (\mathbf{U} + \mathbf{V})(\mathbf{I} + \mathbf{V}^\top \mathbf{V})^{-\frac{1}{2}}$. The polar retraction is a second-order retraction that approximates the exponential mapping up to second-order terms. Consequently, it possesses the following non-expansiveness property and we state the Lemmas and properties that we use throughout the proof, detailed proof of Lemmas can be found in Appendix A.

Lemma 3.4 (Non-expansiveness of polar retraction [5]). *Let $\mathbf{V} \in St(d, r)$, for any point $\mathbf{U} \in \mathcal{T}_{\mathbf{V}}$ with bounded norm, $\|\mathbf{U}\|_F \leq M$, there exists $C \in \mathbb{R}$ such that*

$$\|\mathcal{R}_{\mathbf{V}}(\mathbf{U}) - (\mathbf{V} + \mathbf{U})\|_F \leq C\|\mathbf{U}\|_F^2. \quad (11)$$

Lemma 3.5 (Lipschitz type inequality [5]). *Let $\mathbf{U}, \mathbf{V} \in St(d, r)$. If a function ψ is L -Lipschitz smooth in $\mathbb{R}^{d \times r}$, the following inequality holds:*

$$|\psi(\mathbf{V}) - (\psi(\mathbf{U}) + \langle P_{\mathcal{T}_{\mathbf{U}}}(\nabla \psi(\mathbf{U})), \mathbf{V} - \mathbf{U} \rangle)| \leq \frac{L_g}{2} \|\mathbf{V} - \mathbf{U}\|_F^2$$

where $L_g = L + G$ with $G := \max_{\mathbf{U} \in St(d, r)} \|\nabla \psi(\mathbf{U})\|_2$.

Using Assumption 3.1 and Lemma 3.2 we introduce the following Lemmas to be used in the proof.

Lemma 3.6 (Lipschitz smoothness and bounded gradients with respect to σ). *For all $i \in [m]$ and $\mathbf{U}_i, \mathbf{V} \in St(d, r)$, within the domain $\sigma \in [\omega \sqrt{\frac{2\xi}{d}}, \infty]$, the function $f_i^{\text{pca}}(\mathbf{U}_i, \mathbf{V}, \sigma)$ is L_σ -Lipschitz smooth with respect to σ with constants*

$$L_\sigma := \frac{d^2}{2\xi\omega^2} + \frac{3d^2}{2\xi\omega^4} + \frac{3d^2}{\xi^2\omega^4}.$$

Lemma 3.7 (Lipschitz smoothness and bounded gradients with respect to \mathbf{U}_i). *The function $f_i^{\text{pca}}(\mathbf{U}_i, \mathbf{V}, \sigma)$ is L_U -Lipschitz smooth with respect to \mathbf{U}_i and $\|\nabla f_i^{\text{pca}}(\mathbf{U}_i, \mathbf{V}, \sigma)\|_2 \leq G_U$ for all $i \in [m]$ with constants*

$$L_U := \frac{n}{2} \left(\frac{1}{\sigma_\epsilon^2} + \frac{G_{\text{max,op}}}{\sigma_\epsilon^4} + \left(1 + \frac{2G_{\text{max,op}}}{\sigma_\epsilon^2} \right) \frac{2}{\sigma_\epsilon^4} \right) + \frac{d}{\xi\omega^2},$$

$$G_U := \frac{n}{2} \left(\frac{G_{\text{max,op}}}{\sigma_\epsilon^4} + \frac{1}{\sigma_\epsilon^2} \right) + \frac{d}{\xi\omega^2}.$$

Lemma 3.8 (Lipschitz smoothness and bounded gradients with respect to \mathbf{V}). *The function $f^{\text{pca}}(\{\mathbf{U}_i\}_i, \mathbf{V}, \sigma)$ is L_V -Lipschitz smooth with respect to \mathbf{V} and $\|\nabla f^{\text{pca}}(\{\mathbf{U}_i\}_i, \mathbf{V}, \sigma)\|_2 \leq G_V$ with constants*

$$L_V := \frac{12d}{\xi\omega^2},$$

$$G_V := \frac{3d}{\xi\omega^2}.$$

Lemma 3.9 (Lipschitz continuity of $\frac{\partial}{\partial \sigma} f_i^{\text{pca}}(\mathbf{U}, \mathbf{V}, \sigma)$ with respect to \mathbf{U}, \mathbf{V}). *The function $\frac{\partial}{\partial \sigma} f_i^{\text{pca}}(\mathbf{U}, \mathbf{V}, \sigma)$ is $L_U^{(\sigma)}$ -Lipschitz continuous with respect to \mathbf{U} and $L_V^{(\sigma)}$ -Lipschitz continuous with respect to \mathbf{V} with*

$$L_U^{(\sigma)} = \frac{\sqrt{2d^3}}{\omega^3 \sqrt{\xi^3}},$$

$$L_V^{(\sigma)} = \frac{2\sqrt{d^3}}{\omega^3 \sqrt{2\xi^3}}.$$

Before showing the convergence results, we define the following terms. Let

$$\begin{aligned}
C_{\eta_1} &= C_1 G_1 + \frac{(L_U + G_U)(C_1^2 G_1^2 + 1)}{2}, \\
C_{\eta_2} &= C_2 G_2 + \frac{(L_V + G_V)(C_2^2 G_2^2 + 1)}{2}, \\
G_1 &= 2G_U \sqrt{d}, \\
G_2 &= 2G_V \sqrt{d}.
\end{aligned} \tag{12}$$

with some constants C_1, C_2 given by Lemma 3.4 and G_U, G_V given in Lemma 3.7, 3.8. Given the above results, we can obtain overall sufficient decrease as follows,

Lemma 3.10 (Sufficient Decrease). *At any iteration t , we have*

$$\begin{aligned}
& f^{\text{pca}}(\{\mathbf{U}_{i,t}\}_i, \mathbf{V}_t, \sigma_t) - f^{\text{pca}}(\{\mathbf{U}_{i,t-1}\}_i, \mathbf{V}_{t-1}, \sigma_{t-1}) \\
& \leq \left(-\eta_1 + C_{\eta_1} \eta_1^2 + \eta_3 (L_U^{(\sigma)})^2 \right) \frac{1}{m} \sum_{i=1}^m \left\| P_{\mathcal{T}_{\mathbf{U}_{i,t-1}}} \left(\nabla_{\mathbf{U}_{i,t-1}} f_i^{\text{pca}}(\mathbf{U}_{i,t-1}, \mathbf{V}_{t-1}, \sigma_{t-1}) \right) \right\|_F^2 \\
& \quad + \left(-\eta_2 + C_{\eta_2} \eta_2^2 + \eta_3 (L_V^{(\sigma)})^2 \right) \left\| P_{\mathcal{T}_{\mathbf{V}_{t-1}}} \left(\nabla_{\mathbf{V}_{t-1}} f^{\text{pca}}(\{\mathbf{U}_{i,t}\}_i, \mathbf{V}_{t-1}, \sigma_{t-1}) \right) \right\|_F^2 \\
& \quad + \left(\frac{-\eta_3 + \eta_3^2 L_\sigma}{2} \right) \left[\frac{\partial}{\partial \sigma_{t-1}} f^{\text{pca}}(\{\mathbf{U}_{i,t-1}\}_i, \mathbf{V}_{t-1}, \sigma_{t-1}) \right]^2.
\end{aligned}$$

Proof outline of Theorem 3.3. We show that a lower bound on σ_t is obtained with a proper initialization of σ_0 and we can further derive the Lipschitz constants of the loss function (4). The sufficient decrease of the loss function w.r.t. \mathbf{U}_i, \mathbf{V} , and σ (Lemma 3.10) are derived individually using non-expansiveness of polar retraction (Lemma 3.4) and Lipschitz type inequality (Lemma 3.5). After the sufficient decrease, we show that by choosing $\eta_1 = \min\{\frac{1}{3C_{\eta_1}}, 1\}$, $\eta_2 = \min\{\frac{1}{3C_{\eta_2}}, 1\}$, and $\eta_3 = \min\left\{\frac{\eta_1}{3(L_U^{(\sigma)})^2}, \frac{\eta_2}{3(L_V^{(\sigma)})^2}, \frac{1}{bL_\sigma}\right\}$, we have. The proofs of Lemmas can be found in Appendix A. Technical challenges in this proof are to control the error due to projections, utilize the lower bound on σ to avoid non-smoothness, and use the Lipschitz continuity of the gradients to combine updates on PCs with the update on σ .

3.2 Personalized Adaptive AEs: ADEPT-AE

Algorithm 2 shows the alternating gradient descent training procedure for personalized adaptive AEs. At the beginning of local iterations (**line 8**) the clients receive the global model and σ^5 terms then do local updates on θ_i (**line 10**). At the end of local iterations, the client updates the global model and variance term using its personalized model **lines 12,13** and sends them to the server where it is aggregated and broadcast again (**lines 21-23**).

Assumption 3.11. The loss function $f_i^{(\text{ae})}(\{\theta_i\}, \mu, \sigma)$ is L_θ -smooth w.r.t. individual $\{\theta_i\}$, L_μ -smooth w.r.t. μ and L_σ -smooth w.r.t. σ . Note that only the first one is an assumption, second and third ones are derived from the fact that σ is lower bounded when initialized properly (Appendix B).

Define $\mathbf{g}_{i,t}^\theta = \nabla_{\theta_{i,t-1}} f_i^{\text{ae}}(\theta_{i,t-1}, \mu_{t-1}, \sigma_{t-1})$, $\mathbf{g}_t^\mu = \nabla_{\mu_{t-1}} f^{\text{ae}}(\{\theta_{i,t}\}_i, \mu_{t-1}, \sigma_{t-1})$, $\mathbf{g}_t^\sigma = \frac{\partial f(\{\theta_{i,t}\}_i, \mu_{t-1}, \sigma_{t-1})}{\partial \sigma_{t-1}}$. For Algorithm 2, we obtain the following convergence upper bound for finding a first-order stationary point.

Theorem 3.12 (Convergence of ADEPT-AE (Algorithm 2)). *Let us define $G_t = (\frac{1}{m} \sum_{i=1}^m \|\mathbf{g}_{i,t}^\theta\|^2) + \|\mathbf{g}_t^\mu\|^2 + (g_t^\sigma)^2$. Then, by choosing $\eta_1 = \frac{1}{L_\theta}$, $\eta_2 = \frac{1}{L_\sigma + L_\sigma^{(\mu)^2}}$, and $\eta_3 = \min\{1, \frac{1}{L_\mu}\}$, we have*

$$\min_{t \in [T], \tau | t} \{G_t\} \leq \frac{\max\{L_\theta, L_\sigma + L_\sigma^{(\mu)^2}, L_\mu, 1\} \Delta_T^{\text{ae}}}{R},$$

where $R = T/\tau$ is the number of communication rounds, $\Delta_T^{\text{ae}} = f^{\text{ae}}(\{\theta_{i,0}\}_i, \mu_0, \sigma_0) - f^{\text{ae}}(\{\theta_{i,T}\}_i, \mu_T, \sigma_T)$, and the constants can be found in lemma 3.15.

⁵In the experiments we use individual variance terms for each weight that is $\sigma \in \Theta$ which only has a constant effect on convergence.

Algorithm 2 ADEPT-AE Algorithm

Input: Number of iterations T , learning rates (η_1, η_2, η_3) , number of local iterations τ

```
1: Init local models  $\{\theta_{i,0}\}_{i=1}^m$ , global model  $\mu_0$ , and  $\sigma_0$ .
2: On server:
3: Broadcast  $\mu_0, \sigma_0$  to all clients
4: for  $t = 1$  to  $T$  do
5:   On Clients:
6:   for  $i = 1$  to  $m$  do
7:     if  $\tau$  divides  $t - 1$  then
8:       Receive  $\mu_{t-1}, \sigma_{t-1}$ 
9:     end if
10:     $\theta_{i,t} = \theta_{i,t-1} - \eta_1 \nabla_{\theta_{i,t-1}} f_i^{\text{ae}}(\theta_{i,t-1}, \mu_{t-1}, \sigma_{t-1})$ 
11:    if  $\tau$  divides  $t$  then
12:       $\mu_{i,t} = \mu_{t-1} - \eta_2 \nabla_{\mu_{t-1}} f_i^{\text{ae}}(\theta_{i,t}, \mu_{t-1}, \sigma_{t-1})$ 
13:       $\sigma_{i,t} = \sigma_{t-1} - \eta_3 \nabla_{\sigma_{t-1}} f_i^{\text{ae}}(\theta_{i,t}, \mu_{t-1}, \sigma_{t-1})$ 
14:      Send  $\mu_{i,t}, \sigma_{i,t}$  to server
15:    else
16:       $\mu_t = \mu_{t-1}, \sigma_t = \sigma_{t-1}$ 
17:    end if
18:  end for
19:  At the Server:
20:  if  $\tau$  divides  $t$  then
21:    Receive  $\{\mu_{i,t}\}_{i=1}^m$  and  $\{\sigma_{i,t}\}_{i=1}^m$ 
22:     $\mu_t = \frac{1}{m} \sum_{i=1}^m \mu_{i,t}, \sigma_t = \frac{1}{m} \sum_{i=1}^m \sigma_{i,t}$ 
23:    Broadcast  $\mu_t, \sigma_t$  to all clients
24:  end if
25: end for
```

Output: Personalized autoencoders $\{\theta_{1,T}, \dots, \theta_{m,T}\}$.

Remark 3.13. By examining the multiplicative constants within the bounds specified in Theorems 3.3 and 3.12, we note a consistent observation: σ exhibits an inverse relationship with convergence speed. A higher σ , whether resulting from a large value of ξ or inherent heterogeneity in the setting, can expedite the convergence process. Essentially, a large σ diminishes collaboration, allowing the model to fit quickly due to a reduced effective number of samples. Conversely, a smaller σ promotes collaboration and may augment the effective sample count. Observe that faster convergence does not necessarily imply a superior generalization error. Consequently, in our experiments, opting for a high value of σ_0 facilitates fast convergence in the initial stages, while still allowing flexibility for adjustments to yield a superior generalization error.

3.2.1 Proof outline of Theorem 3.12

Here we present a proof outline for Theorem 3.12, detailed proof of lemmas and intermediate steps is provided in Appendix B. We start with an assumption that is necessary to have smoothness w.r.t. σ , and a lemma indicating Lipschitz properties of the loss function. The assumption is equivalent to having an upper bound over the gradient w.r.t. σ , which is a standard assumption for model parameters.

Assumption 3.14. Assume that there exists some $B > 0$ such that for the weights of the autoencoders, we have $\|\mu\| \leq B$ and $\|\theta_i\| \leq B$ for all $i \in [m]$.

Now we show the Lipschitzness properties of the loss function.

Lemma 3.15. *The loss function $f_i^{\text{ae}}(\boldsymbol{\theta}_i, \boldsymbol{\mu}, \sigma)$ is L_μ -smooth w.r.t. $\boldsymbol{\mu}$ and L_σ -smooth w.r.t. σ with*

$$L_\mu = \frac{d_\theta}{2\xi\omega^2}$$

$$L_\sigma = \frac{3\xi d_\theta^2}{2\xi^2\omega^4} + \frac{3d_\theta^2 B^2}{\xi^2\omega^4} + \frac{d_\theta^2}{2\xi\omega^2}.$$

Also, we have

$$\|\nabla_{\boldsymbol{\mu}} f_i^{\text{ae}}(\boldsymbol{\theta}, \boldsymbol{\mu}, \sigma_1) - \nabla_{\boldsymbol{\mu}} f_i^{\text{ae}}(\boldsymbol{\theta}, \boldsymbol{\mu}, \sigma_2)\| \leq L_\sigma^{(\boldsymbol{\mu})} |\sigma_1 - \sigma_2|$$

with

$$L_\sigma^{(\boldsymbol{\mu})} = \frac{B\sqrt{d_\theta^3}}{\omega^3\sqrt{2\xi^3}}.$$

Sufficient decrease when τ divides t At communication round time steps we have the following decrease property,

$$f^{\text{ae}}(\{\boldsymbol{\theta}_{i,t}\}, \boldsymbol{\mu}_t, \sigma_t) - f^{\text{ae}}(\{\boldsymbol{\theta}_{i,t-1}\}, \boldsymbol{\mu}_{t-1}, \sigma_{t-1}) \leq \left(-\eta_1 + \eta_1^2 \frac{L_\theta}{2}\right) \left(\frac{1}{m} \sum_{i=1}^m \|\nabla_{\boldsymbol{\theta}_{i,t-1}} f_i^{\text{ae}}(\boldsymbol{\theta}_{i,t-1}, \boldsymbol{\mu}_{t-1}, \sigma_{t-1})\|^2\right)$$

$$+ \left(-\eta_2 + \eta_2^2 \frac{L_\sigma + L_\sigma^{(\boldsymbol{\mu})^2}}{2}\right) (g_t^\sigma)^2 + \left(-\frac{\eta_3}{2} + \frac{L_\mu \eta_3^2}{2}\right) \|\mathbf{g}_t^\mu\|^2. \quad (13)$$

Sufficient decrease when τ does not divide t At time steps that are not communication rounds we simply have decreased due to the updates of $\{\boldsymbol{\theta}_i\}$, that is,

$$f^{\text{ae}}(\{\boldsymbol{\theta}_{i,t}\}, \boldsymbol{\mu}_t, \sigma_t) - f^{\text{ae}}(\{\boldsymbol{\theta}_{i,t-1}\}, \boldsymbol{\mu}_{t-1}, \sigma_{t-1}) = f^{\text{ae}}(\{\boldsymbol{\theta}_{i,t}\}, \boldsymbol{\mu}_{t-1}, \sigma_{t-1}) - f^{\text{ae}}(\{\boldsymbol{\theta}_{i,t-1}\}, \boldsymbol{\mu}_{t-1}, \sigma_{t-1})$$

$$= \frac{1}{m} \sum_{i=1}^m (f_i^{\text{ae}}(\boldsymbol{\theta}_{i,t}, \boldsymbol{\mu}_{t-1}, \sigma_{t-1}) - f_i^{\text{ae}}(\boldsymbol{\theta}_{i,t-1}, \boldsymbol{\mu}_{t-1}, \sigma_{t-1}))$$

$$\leq \left(-\eta_1 + \eta_1^2 \frac{L_\theta}{2}\right) \left(\frac{1}{m} \sum_{i=1}^m \|\nabla_{\boldsymbol{\theta}_{i,t-1}} f_i^{\text{ae}}(\boldsymbol{\theta}_{i,t-1}, \boldsymbol{\mu}_{t-1}, \sigma_{t-1})\|^2\right).$$

By choosing, $\eta_1 = \frac{1}{L_\theta}$, $\eta_2 = \frac{1}{L_\sigma + L_\sigma^{(\boldsymbol{\mu})^2}}$, $\eta_3 = \min\{1, \frac{1}{L_\mu}\}$, and by averaging over time steps while combining two type of decrease, we obtain the final bound.

Proof outline of Theorem 3.12. Since the form of the adaptation in the loss function is similar to the PCA loss function, the lower bound on sigma (Lemma 3.2) holds for ADEPT-AE as well. We utilize the lower bound to derive the Lipschitz smoothness constants with respect to $\boldsymbol{\mu}$ and $\boldsymbol{\sigma}$ (Lemma 3.15), and the Lipschitz smoothness constant with respect to $\boldsymbol{\theta}$ is stated in Assumption 3.11. Then, we derive the sufficient decrease with respect to $\boldsymbol{\theta}$, $\boldsymbol{\mu}$, and $\boldsymbol{\sigma}$ with the Lipschitz constants. However, we have multiple local iterations for one communication round in ADEPT-AE. Thus, we have to deal with the sufficient decrease separately depending on whether the round is a communication round. With careful derivation under the two cases, we can combine them in the end and get to our Theorem 3.12.

Remark 3.16. In the experiments for ADEPT-AE, we treat sigma as a vector $\boldsymbol{\sigma} \in \mathbb{R}^{d_\theta}$ so that each weight in the models can learn its own σ_j instead of sharing one σ across all the weights. The convergence for the modified algorithm is almost identical to the proof here. Moreover, it can be shown that for the Lipschitz smoothness constant L_σ , the dependence on the dimension in the numerators becomes d_θ instead of d_θ^2 . This is because our lower bound in Lemma 3.2 will not depend on d_θ in this case.

Algorithm 3 Personalized Adaptive Diffusion Model: ADEPT-DGM

Input: Number of iterations T , learning rates (η_2, η_1, η_3) , number of local iterations τ , sample corruption range $\gamma \in \mathbb{Z}^+$

```
1: Init local models  $\{\theta_{i,0}\}_{i=1}^m$ , global model  $\mu_0$ , and  $\sigma_0$ .
2: On server:
3: Broadcast  $\mu_0, \sigma_0$  to all clients
4: for  $t = 1$  to  $T$  do
5:   On Clients:
6:   for  $i = 1$  to  $m$  do
7:     if  $\tau$  divides  $t - 1$  then
8:       Receive  $\mu_{t-1}, \sigma_{t-1}$ 
9:     end if
10:    Sample noise amount  $\alpha_i \in \text{Uniform}[1, \dots, \gamma]$  independently for each sample and construct  $\alpha = [\alpha_1, \dots, \alpha_n]$ 
11:     $\theta_{i,t} = \theta_{i,t-1} - \eta_1 \nabla_{\theta_{i,t-1}} f_{i,\alpha}^{\text{df}}(\theta_{i,t-1}, \mu_{t-1}, \sigma_{t-1})$ 
12:    if  $\tau$  divides  $t$  then
13:       $\mu_{i,t} = \mu_{t-1} - \eta_2 \nabla_{\mu_{t-1}} f_{i,\alpha}^{\text{df}}(\theta_{i,t}, \mu_{t-1}, \sigma_{t-1})$ 
14:       $\sigma_{i,t} = \sigma_{t-1} - \eta_3 \frac{\partial}{\partial \sigma_{t-1}} f_{i,\alpha}^{\text{df}}(\theta_{i,t}, \mu_{t-1}, \sigma_{t-1})$ 
15:      Send  $\mu_{i,t}, \sigma_{i,t}$  to server
16:    else
17:       $\mu_t = \mu_{t-1}, \sigma_t = \sigma_{t-1}$ 
18:    end if
19:  end for
20:  At the Server:
21:  if  $\tau$  divides  $t$  then
22:    Receive  $\{\mu_{i,t}\}_{i=1}^m$  and  $\{\sigma_{i,t}\}_{i=1}^m$ 
23:     $\mu_t = \frac{1}{m} \sum_{i=1}^m \mu_{i,t}, \sigma_t = \frac{1}{m} \sum_{i=1}^m \sigma_{i,t}$ 
24:    Broadcast  $\mu_t, \sigma_t$  to all clients
25:  end if
26: end for
Output: Personalized autoencoders  $\{\theta_{1,T}, \dots, \theta_{m,T}\}$ .
```

4 Personalized Generation through Adaptive Diffusion Models: ADEPT-DGM

In Algorithm 3, the main change compared to ADEPT-AE is that we input a corrupted sample to the network during the forward pass (**line 11**) to train it as a denoiser. Accordingly, $f_{i,\alpha}^{\text{df}}(\theta_i, \mu, \sigma) := \|\phi(\mathbf{X}(1 - \alpha) + \mathbf{Z}\alpha; \theta_i, \alpha) - \mathbf{X}\|^2 + \frac{2\xi + \|\mu - \theta_i\|^2}{2\sigma^2} + d \log \sigma$, where α is the randomly sampled noise amount.

Remark 4.1. It is easy to see that one can prove a convergence result identical to Theorem 3.12 for ADEPT-DGM Algorithm 3.

As an illustration of the effectiveness of personalized diffusion model learning, we analyze a simple personalized Gaussian distribution generation problem, i.e., client- i 's target distribution is a Gaussian distribution $p(\mathbf{x}|\theta_i) = \mathcal{N}(\mathbf{x}; \theta_i, \sigma_0^2 \mathbf{I}_d)$. In the following, we first introduce some details of the canonical denoising diffusion model for Gaussian target distribution and analyze the improvement of collaboration in the proposed personalized algorithm.

Diffusion model with Gaussian target distribution: When the desired distribution is $\mathcal{N}(\mathbf{x}; \theta, \sigma_0^2 \mathbf{I}_d)$, the diffusion process (7) is a Gaussian process and the drift term for the reverse-time process (8) is a linear function, i.e., $\nabla \ln p_{\mathbf{x}_{T-t}}(\mathbf{x}_t^\leftarrow) = -\frac{\mathbf{x}_t^\leftarrow - \theta}{\sigma_0^2 + t}$. The time-reversed process is

$$d\mathbf{x}_t^\leftarrow = \nabla \ln p_{\mathbf{x}_{T-t}}(\mathbf{x}_t^\leftarrow) dt + d\mathbf{w}_t^\leftarrow, \mathbf{x}_0^\leftarrow \sim \mathcal{N}(\theta, (\sigma_0^2 + T)\mathbf{I}_d). \quad (14)$$

Without the knowledge of θ , we approximate the score function by a neural network of $\phi(\mathbf{x}; \hat{\theta}, t) = -\frac{\mathbf{x} - \hat{\theta}}{\sigma_0^2 + t}$ and approximate the initial distribution of the time-reversed process $\mathcal{N}(\theta, (\sigma_0^2 + T)\mathbf{I}_d)$ by $\mathcal{N}(\mathbf{0}, (\sigma_0^2 + T)\mathbf{I}_d)$. The learned/approximated time-reversed process is then

$$d\mathbf{x}_t^\leftarrow = -\frac{\mathbf{x} - \hat{\theta}}{\sigma_0^2 + t} dt + d\mathbf{w}_t^\leftarrow, \mathbf{x}_0^\leftarrow \sim \mathcal{N}(\mathbf{0}, (\sigma_0^2 + T)\mathbf{I}_d). \quad (15)$$

The following lemma characterizes the difference between the generation distribution and the target distribution.

Lemma 4.2. *The output distribution $p_{\mathbf{x}_T^\leftarrow|\hat{\theta}}$ of the learned reversed-time process (15) satisfies,*

$$D_{KL}(p_{\mathbf{x}|\theta} \| p_{\mathbf{x}_T^\leftarrow|\hat{\theta}}) = \left\| \theta - \hat{\theta} + \frac{\sigma_0^2}{\sigma_0^2 + T} \hat{\theta} \right\|^2, \quad (16)$$

where D_{KL} is the Kullback-Leibler divergence and $p_{\mathbf{x}|\theta} = \mathcal{N}(\mathbf{x}; \theta, \sigma_0^2 \mathbf{I}_d)$ is the target distribution.

The lemma shows that the KL-divergence between target distribution and the learned distribution is measured by the difference between θ and $\hat{\theta}$ a bias term $\frac{\sigma_0^2}{\sigma_0^2 + T} \hat{\theta}$ due to the initial distribution mismatch of the time-reversed process.

It is straightforward to verify that for $\phi(\mathbf{x}; \hat{\theta}, t) = -\frac{\mathbf{x} - \hat{\theta}}{\sigma_0^2 + t}$, training with dataset $\mathbf{X} = (\mathbf{x}_1, \dots, \mathbf{x}_n)$ by maximizing ELBO (9) has a closed-form sample-mean solution, i.e., $\hat{\theta} = \arg \max_{\theta} ELBO_{\theta}(\mathbf{X}) = \frac{\sum_{j=1}^n \mathbf{x}_j}{n}$. Since the data are i.i.d. sampled from $\mathcal{N}(\theta, \sigma_0^2 \mathbf{I}_d)$, we have $\mathbb{E}[D_{KL}(p_{\mathbf{x}|\theta} \| p_{\mathbf{x}_T^\leftarrow|\hat{\theta}})] = \frac{\sigma_0^2}{n}$, when omitting the initial distribution bias by $T \rightarrow \infty$. It can be viewed as personalized training without collaboration and in the following, we show that the proposed personalized training with collaboration can improve over this.

Personalized denoising diffusion model with Gaussian targets: The local dataset \mathbf{X}_i of client- i sampled i.i.d. from a target Gaussian distribution $P(\mathbf{x}|\theta_i) = \mathcal{N}(\mathbf{x}; \theta_i, \sigma_0^2 \mathbf{I}_d)$, and the population distribution is also Gaussian with $P(\theta|\Gamma_*) = \mathcal{N}(\theta; \mu_*, \sigma_*^2 \mathbf{I}_d)$. Note that we conduct analysis for a fixed unknown population distribution parameterized by $\Gamma_* = (\mu_*, \sigma_*)$, though the proposed loss function and algorithm follows a Hierarchical Bayesian model as in Section 2.3.

Lemma 4.3 (Personalized estimation). *For the parameterized score function $\phi(\mathbf{x}; \theta, t) = -\frac{\mathbf{x} - \theta}{\sigma_0^2 + t}$, the optimal solution to (10) is*

$$\hat{\mu} = \frac{\sum_{i=1}^m \sum_{j=1}^n \mathbf{x}_{ij}}{mn}$$

$$\hat{\theta}_i = \frac{n\alpha\hat{\sigma}^2}{n\alpha\hat{\sigma}^2 + 1} \frac{\sum_{j=1}^n \mathbf{x}_{ij}}{n} + \frac{\hat{\mu}}{n\alpha\hat{\sigma}^2 + 1},$$

where $\alpha = \frac{1}{\sigma_0^2} - \frac{1}{\sigma_0^2 + T}$ and $\hat{\sigma}^2$ satisfies $\hat{\sigma}^2 = \frac{2\xi}{d} + s^2 \left(\frac{n\alpha\hat{\sigma}^2}{n\alpha\hat{\sigma}^2 + 1} \right)^2$ with $s^2 = \frac{\sum_{i=1}^m \|\hat{\mu} - \frac{1}{n} \sum_{j=1}^n \mathbf{x}_{ij}\|^2}{md}$.

Remark 4.4. We note that the global optimum model is the average of average samples of each client. The personalized optimum model is interpolation of local estimate and the true global model. The interpolation coefficient depends on the heterogeneity (large σ skews the result towards the local estimate and low σ skews it towards true global model). A large amount of local samples n decreases the reliance on μ . These observations are in parallel with findings in [28] on mean estimation.

Theorem 4.5 (Condition for performance improvement). *Consider an asymptotic regime that $m \rightarrow \infty$ and $T \rightarrow \infty$. Compared to training without collaboration, the solution of $(\{\hat{\theta}_i\}, \hat{\mu}, \hat{\sigma}^2)$ in Lemma 4.3 improves the averaged KL-divergence $\frac{1}{m} \sum_{i=1}^m D_{KL}(p_{\mathbf{x}|\theta_i} \| p_{\mathbf{x}_T^\leftarrow|\hat{\theta}_i})$ by a factor of $\left(\frac{2\hat{\sigma}^2 + \sigma_0^2/n - \sigma_*^2}{\hat{\sigma}^2 + \sigma_0^2/n} \right) \frac{\sigma_0^2/n}{\hat{\sigma}^2 + \sigma_0^2/n} \frac{\sigma_0^2}{n}$, when $\hat{\sigma}^2 > \frac{\sigma_*^2}{2} - \frac{\sigma_0^2}{2n}$.*

Corollary 4.6. *Under the same setting as in Theorem 4.5, choosing $\xi \geq \frac{3d\sigma_0^2}{2n}$ guarantees strict improvement of collaboration for any population distribution $\mathcal{N}(\mu_*, \sigma_* \mathbf{I}_d)$.*

Remark 4.7. Note that if our estimate $\hat{\sigma}^2$ of the population variance is accurate, *i.e.*, $\hat{\sigma}^2 = \sigma_*^2$, then collaboration always improves over only using local data for personalized generation; and in fact the collaboration gain is the largest. In this case, the gain is larger when the number of local samples is relatively small. However, if the estimate is inaccurate, one could, in principle be better off without collaboration. However, by setting the hyperparameter $\xi \geq \frac{3d\sigma_0^2}{2n}$, we can ensure that our estimate $\hat{\sigma}^2 \geq \frac{1}{2}(\sigma_*^2 - \sigma_0^2/n)$, ensuring that collaboration is useful.

4.1 Proofs

Proof of Lemma 4.2. Let $\beta_t = \frac{1}{T-t+\sigma_0^2}$. For stochastic differential equation

$$d\mathbf{x}_t^\leftarrow + \beta_t(\mathbf{x}_t^\leftarrow - \hat{\boldsymbol{\theta}})dt = d\mathbf{w}_t, \quad \mathbf{x}_0^\leftarrow \sim \mathcal{N}(0, (\sigma_0^2 + T)\mathbf{I}_d),$$

we have

$$\begin{aligned} d(e^{\int_0^t \beta_s ds}(\mathbf{x}_t^\leftarrow - \hat{\boldsymbol{\theta}})) &= e^{\int_0^t \beta_s ds} d\mathbf{x}_t^\leftarrow + e^{\int_0^t \beta_s ds} \beta_t(\mathbf{x}_t^\leftarrow - \hat{\boldsymbol{\theta}})dt \\ &= e^{\int_0^t \beta_s ds} (d\mathbf{x}_t^\leftarrow + \beta_t(\mathbf{x}_t^\leftarrow - \hat{\boldsymbol{\theta}})dt) = e^{\int_0^t \beta_s ds} d\mathbf{w}_t. \end{aligned}$$

Note that

$$e^{\int_0^t \beta_s ds} = e^{\int_0^t \frac{1}{T-s+\sigma_0^2} ds} = e^{\ln(T+\sigma_0^2) - \ln(T-t+\sigma_0^2)} = \frac{T + \sigma_0^2}{T - t + \sigma_0^2}$$

and

$$\int_0^T e^{2\int_0^t \beta_s ds} dt = \int_0^T \frac{(T + \sigma_0^2)^2}{(T + \sigma_0^2 - t)^2} dt = (T + \sigma_0^2)^2 \left(\frac{1}{\sigma_0^2} - \frac{1}{T + \sigma_0^2} \right) = \left(1 + \frac{T}{\sigma_0^2} \right) T.$$

It then follows that

$$e^{\int_0^T \beta_s ds}(\mathbf{x}_T^\leftarrow - \hat{\boldsymbol{\theta}}) - (\mathbf{x}_0^\leftarrow - \hat{\boldsymbol{\theta}}) \sim \mathcal{N}\left(0, \int_0^T e^{2\int_0^t \beta_s ds} dt\right) = \mathcal{N}\left(0, \left(1 + \frac{T}{\sigma_0^2}\right) T\right),$$

and equivalently

$$\mathbf{x}_T^\leftarrow = \hat{\boldsymbol{\theta}} + \frac{\sigma_0^2}{\sigma_0^2 + T}(\mathbf{x}_0^\leftarrow - \hat{\boldsymbol{\theta}}) + \sqrt{\frac{\sigma_0^2 T}{\sigma_0^2 + T}}\boldsymbol{\epsilon},$$

where $\boldsymbol{\epsilon} \sim \mathcal{N}(0, \mathbf{I}_d)$.

Since $\mathbf{x}_0^\leftarrow \sim \mathcal{N}(0, (\sigma_0^2 + T)\mathbf{I}_d)$, we have $p_{\mathbf{x}_T^\leftarrow|\hat{\boldsymbol{\theta}}} = \mathcal{N}\left(\hat{\boldsymbol{\theta}} - \frac{\sigma_0^2}{\sigma_0^2 + T}\hat{\boldsymbol{\theta}}, \sigma_0^2\mathbf{I}_d\right)$. The KL-divergence between the target distribution $p_{\mathbf{x}|\boldsymbol{\theta}} = \mathcal{N}(\boldsymbol{\theta}, \sigma_0^2\mathbf{I}_d)$ and $p_{\mathbf{x}_T^\leftarrow|\hat{\boldsymbol{\theta}}}$ can then be calculated as $\left\| \boldsymbol{\theta} - \hat{\boldsymbol{\theta}} + \frac{\sigma_0^2}{\sigma_0^2 + T}\hat{\boldsymbol{\theta}} \right\|^2$. \square

Proof of Lemma 4.3. The parameterized score function is $\boldsymbol{\phi}(x; \boldsymbol{\theta}, t) = -\frac{\mathbf{x} - \boldsymbol{\theta}}{\sigma_0^2 + t}$. Note that $\nabla_{\mathbf{x}_t} \ln p_{\mathbf{x}_t|\mathbf{x}_0}(\mathbf{x}_t|\mathbf{x}_0) = -\frac{\mathbf{x}_t - \mathbf{x}_0}{t}$ since $\mathbf{x}_t|\mathbf{x}_0 \sim \mathcal{N}(\mathbf{x}_0, t\mathbf{I}_d)$. The training loss of (10) can then be written as

$$\frac{1}{m} \sum_{i=1}^m \sum_{j=1}^n \int_{t=0}^T \mathbb{E}_{\boldsymbol{\epsilon} \sim \mathcal{N}(0, \mathbf{I}_d)} \left[\frac{1}{2} \left\| \boldsymbol{\phi}(\mathbf{x}_{ij} + \sqrt{t}\boldsymbol{\epsilon}; \boldsymbol{\theta}_j, t) + \boldsymbol{\epsilon}/\sqrt{t} \right\|^2 \right] dt + \sum_{j=1}^m \frac{2\xi + \|\boldsymbol{\theta}_j - \boldsymbol{\mu}\|^2}{2\sigma^2} + \frac{d}{2} \ln \sigma^2.$$

Note that

$$\begin{aligned} \int_{t=0}^T \mathbb{E}_{\boldsymbol{\epsilon} \sim \mathcal{N}(0, \mathbf{I}_d)} [\|\boldsymbol{\phi}(\mathbf{x}_{ij} + \sqrt{t}\boldsymbol{\epsilon}; \boldsymbol{\theta}, t) + \boldsymbol{\epsilon}/\sqrt{t}\|^2] dt &= \int_{t=0}^T \mathbb{E}_{\boldsymbol{\epsilon} \sim \mathcal{N}(0, \mathbf{I}_d)} \left[\left\| -\frac{\mathbf{x}_{ij} + \sqrt{t}\boldsymbol{\epsilon} - \boldsymbol{\theta}}{\sigma_0^2 + t} + \frac{\boldsymbol{\epsilon}}{\sqrt{t}} \right\|^2 \right] dt \\ &= \int_0^T \mathbb{E}_{\boldsymbol{\epsilon} \sim \mathcal{N}(0, \mathbf{I}_d)} \left[\left\| \frac{\boldsymbol{\theta} - \mathbf{x}_{ij}}{\sigma_0^2 + t} + \frac{\sigma_0^2}{\sqrt{t}(\sigma_0^2 + t)}\boldsymbol{\epsilon} \right\|^2 \right] dt = \left(\int_0^T \frac{1}{(\sigma_0^2 + t)^2} dt \right) \|\boldsymbol{\theta} - \mathbf{x}_{ij}\|^2 + \text{const.} \end{aligned}$$

Since $\int_0^T \frac{1}{(\sigma_0^2+t)^2} dt = \frac{1}{\sigma_0^2} - \frac{1}{\sigma_0^2+T}$, the optimization of minimizing the training loss is equivalent to

$$\min_{\boldsymbol{\theta}_{1:m}, \boldsymbol{\theta}, \sigma^2} \frac{1}{m} \sum_{i=1}^m \left(\sum_{j=1}^n \frac{\alpha}{2} \|\boldsymbol{\theta}_j - \mathbf{x}_{ij}\|^2 + \frac{2\xi + \|\boldsymbol{\theta}_j - \boldsymbol{\mu}\|^2}{2\sigma^2} \right) + \frac{d}{2} \ln \sigma^2,$$

where $\alpha = \frac{1}{\sigma_0^2} - \frac{1}{\sigma_0^2+T}$. By the KKT condition that

$$\begin{aligned} \sum_{j=1}^n \alpha(\boldsymbol{\theta}_i - \mathbf{x}_{ij}) + \frac{\boldsymbol{\theta}_i - \boldsymbol{\mu}}{\sigma^2} &= 0, \quad \forall i = 1, 2, \dots, m, \\ \boldsymbol{\mu} &= \frac{1}{m} \sum_{i=1}^m \boldsymbol{\theta}_i, \\ -\frac{1}{m} \sum_{i=1}^m \frac{2\xi + \|\boldsymbol{\theta}_j - \boldsymbol{\mu}\|^2}{2\sigma^4} + \frac{d}{2\sigma^2} &= 0, \end{aligned}$$

We thus have

$$\begin{aligned} \hat{\boldsymbol{\mu}} &= \frac{\sum_{i=1}^m \sum_{j=1}^n \mathbf{x}_{ij}}{mn} \\ \hat{\boldsymbol{\theta}}_i &= \frac{n\alpha\hat{\sigma}^2}{n\alpha\hat{\sigma}^2 + 1} \frac{\sum_{j=1}^n \mathbf{x}_{ij}}{n} + \frac{\hat{\boldsymbol{\mu}}}{n\alpha\hat{\sigma}^2 + 1}, \end{aligned}$$

where $\hat{\sigma}^2$ satisfies $\hat{\sigma}^2 = \frac{2\xi}{d} + s^2 \left(\frac{n\alpha\hat{\sigma}^2}{n\alpha\hat{\sigma}^2 + 1} \right)^2$ with $s^2 = \frac{\sum_{i=1}^m \|\hat{\boldsymbol{\mu}} - \frac{1}{n} \sum_{j=1}^n \mathbf{x}_{ij}\|^2}{md}$. \square

Proof of Theorem 4.5. When $m \rightarrow \infty$, $s^2 \rightarrow \frac{\sigma_0^2}{n} + \sigma_*^2$ and $\hat{\boldsymbol{\mu}} \rightarrow \boldsymbol{\mu}_*$, a.s.. $\hat{\sigma}^2$ satisfies

$$\hat{\sigma}^2 = \frac{2\xi}{d} + \left(\frac{\sigma_0^2}{n} + \sigma_*^2 \right) \left(\frac{\hat{\sigma}^2}{\hat{\sigma}^2 + 1/(n\alpha)} \right)^2.$$

Since $\boldsymbol{\theta}_i$ are sampled i.i.d. from a population distribution $\mathcal{N}(\boldsymbol{\mu}_*, \sigma_*^2 \mathbf{I}_d)$. $\alpha = 1/\sigma_0^2$ since $T \rightarrow \infty$. Let $\mathbf{x} \sim \mathcal{N}(\boldsymbol{\theta}, \frac{\sigma_0^2}{n} \mathbf{I}_d)$, $\boldsymbol{\theta} \sim \mathcal{N}(\boldsymbol{\mu}, \sigma^2 \mathbf{I}_d)$, by Lemma 4.2, we have

$$\begin{aligned} \frac{1}{m} \sum_{i=1}^m D_{KL}(p_{\mathbf{x}|\boldsymbol{\theta}_i} \| p_{\mathbf{x}_T|\hat{\boldsymbol{\theta}}_i}) &= \frac{1}{m} \sum_{i=1}^m \left\| \boldsymbol{\theta}_i - \hat{\boldsymbol{\theta}}_i + \frac{\sigma_0^2}{\sigma_0^2 + T} \hat{\boldsymbol{\theta}}_i \right\|^2 \\ &= \mathbb{E} \left[\left\| \boldsymbol{\theta} - \mathbf{x} - \frac{1}{n\alpha\hat{\sigma}^2 + 1} (\boldsymbol{\mu} - \mathbf{x}) \right\|^2 \right] \\ &= \left(\frac{\sigma_0^2/n}{\hat{\sigma}^2 + \sigma_0^2/n} \right)^2 \mathbb{E} [\|\boldsymbol{\theta} - \boldsymbol{\mu}\|^2] + \left(\frac{\hat{\sigma}^2}{\hat{\sigma}^2 + \sigma_0^2/n} \right)^2 \mathbb{E} [\|\boldsymbol{\theta} - \mathbf{x}\|^2] \\ &= \left(\frac{\sigma_0^2/n}{\hat{\sigma}^2 + \sigma_0^2/n} \right)^2 \sigma_*^2 + \left(\frac{\hat{\sigma}^2}{\hat{\sigma}^2 + \sigma_0^2/n} \right)^2 \sigma_0^2/n \\ &= \frac{\sigma_0^2}{n} + \frac{(\sigma_*^2 + \sigma_0^2/n)\sigma_0^2/n}{(\hat{\sigma}^2 + \sigma_0^2/n)^2} \frac{\sigma_0^2}{n} - 2 \frac{\sigma_0^2/n}{\hat{\sigma}^2 + \sigma_0^2/n} \frac{\sigma_0^2}{n} \\ &= \frac{\sigma_0^2}{n} - \left(\frac{2\hat{\sigma}^2 + \sigma_0^2/n - \sigma_*^2}{\hat{\sigma}^2 + \sigma_0^2/n} \right) \frac{\sigma_0^2/n}{\hat{\sigma}^2 + \sigma_0^2/n} \frac{\sigma_0^2}{n} \end{aligned}$$

where the expectation is taken w.r.t. $\mathbf{x}, \boldsymbol{\theta}$.

Since without collaboration, the training of maximizing $ELBO_i$ for client- i leads to parameter $\hat{\boldsymbol{\theta}}_i = \frac{\sum_{j=1}^n \mathbf{x}_{ij}}{n}$ and the KL-divergence between the target distribution and the output distribution is $\frac{\sigma_0^2}{n}$, it follows that collaboration improves the performance as long as $\hat{\sigma}^2 > \frac{\sigma_*^2}{2} - \frac{\sigma_0^2}{2n}$.

The improvement is $\left(\frac{2\hat{\sigma}^2 + \sigma_0^2/n - \sigma_*^2}{\hat{\sigma}^2 + \sigma_0^2/n} \right) \frac{\sigma_0^2/n}{\hat{\sigma}^2 + \sigma_0^2/n} \frac{\sigma_0^2}{n}$ and achieves the maximum when $\hat{\sigma}^2 = \sigma_*^2$, i.e., the learned $\hat{\sigma}^2 = \sigma_*^2$. \square

Proof of Corollary 4.6. Under the same setting as in Theorem 4.5, by Lemma 4.3, we have $\hat{\sigma}^2 = \frac{2\xi}{d} + (\frac{\sigma_0^2}{n} + \sigma_*^2)(\frac{\hat{\sigma}^2}{\hat{\sigma}^2 + \sigma_0^2/n})^2$. Taking $\xi > \frac{2\xi}{d} = \frac{3d\sigma_0^2}{2n}$ gives that $\hat{\sigma}^2 \geq \frac{3\sigma_0^2}{n}$, and thus $\hat{\sigma}^2 > (\frac{\sigma_0^2}{n} + \sigma_*^2)(\frac{\hat{\sigma}^2}{\hat{\sigma}^2 + \sigma_0^2/n})^2 \geq \frac{9}{16}(\frac{\sigma_0^2}{n} + \sigma_*^2) > \frac{\sigma_*^2}{2} - \frac{\sigma_0^2}{2n}$, which guarantees strictly improvement by Theorem 4.5. \square

5 Experiments

5.1 Experimental Setting

In our experiments, our goal is to compare our adaptive personalized unsupervised algorithms with global training (FedAvg, FedAvg+fine-tuning), local training (training individual models without collaboration), and competitive baselines in terms of testing performance under different heterogeneous scenarios. For all experiments, we use 50 clients ($m = 50$) and initialize $\xi = 1e-6$.

ADEPT-PCA: We use synthetic datasets for the experiments of ADEPT-PCA. In the dataset, we first sample a global PC, $\mathbf{V}^* \in St(d, r)$, uniformly on the Steifel manifold. We sample $\{\hat{\mathbf{U}}_i^*\}_{i=1}^m$ where the entries of each $\hat{\mathbf{U}}_i^*$ follows Gaussian distribution with mean being \mathbf{V}^* and variance σ^* . Then, we let $\mathbf{U}_i^* = \mathcal{R}_{\mathbf{V}^*}(P_{\mathcal{T}_{\mathbf{V}^*}}(\hat{\mathbf{U}}_i^*))$ so that it is in the Steifel manifold. Data on each client are then generated by $\mathbf{x} = \mathbf{U}_i^* \mathbf{z} + \epsilon$.

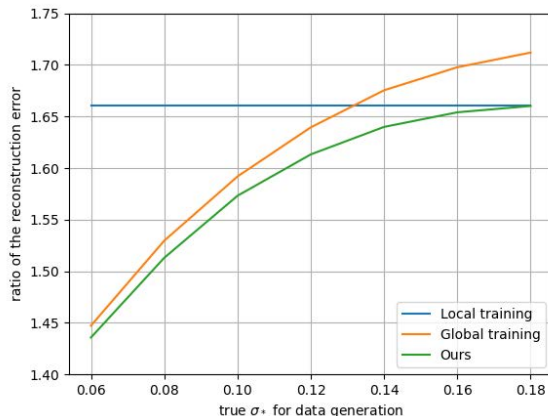


Figure 2: Ratio of the reconstruction error of different methods to the true model w.r.t. different values of σ^* . We have $d = 100$, $r = 20$, $m = 10$, and $n = 20$.

ADEPT-AE: For AEs we do synthetic and real data experiments. In the synthetic experiments from a 0 mean $\sigma_\mu = 0.1$ standard deviation Gaussian, we sample weights for a one-layer decoder $\mu^{d,*}$ with 5 latent dimensionality and 64 output dimensionality. Then by perturbing the weights with another zero-mean Gaussian with σ^* we obtain true personalized decoders, which is used as in (5) to generate 10 local samples across 50 clients. Heterogeneity among clients will depend on σ^* and can be quantified in terms of signal-to-noise ratio as $20 \log_{10} \frac{\sigma_\mu}{\sigma^*}$ dB. For the real data experiments, we use MNIST, Fashion MNIST, and CIFAR-10. To introduce heterogeneity, we distribute the samples such that each client has access to samples from a single class which simulates distinct data distributions for each client (commonly referred as pathological heterogeneity [26]). For MNIST and Fashion MNIST, each client has access to 120 training samples; and for CIFAR-10, 250 samples.

Models. For the synthetic experiments we use a two layer fully connected AE, for MNIST and Fashion MNIST we also use a two layer AE with 784 input dimension with 10 and 20 latent dimensions depending on experiment. For CIFAR-10 we use a symmetric convolutional AE whose input and output layers are convolutional layers with 16 channels, 3 kernel size, 2 stride and no padding; the intermediate layers are fully connected layers that maps 3600 dimensions to latent dimensions. We use 10 and 50 latent dimensionality

Table 1: Total energy captured % averaged over samples and clients in the synthetic experiments.

Method	Heterogeneity (std of noise and SNR)		
	0.05(6dB)	0.025(12dB)	0.01(20dB)
Baseline	88.3 ± 0.5	95.4 ± 0.8	98.6 ± 0.1
ADEPT-AE	87.3 ± 1.1	95.9 ± 0.1	98.7 ± 0.1
Global Training	81.3 ± 0.1	94.3 ± 0.2	98.4 ± 0.4
Local Training	83.2 ± 1.9	83.2 ± 1.9	83.2 ± 1.9

depending on the experiment. We use ReLU activation function after the first layer and sigmoid after the last layer.

Training and hyper-parameters. For the synthetic experiments we don't do local iterations and just do distributed training. For the other experiments, we do 20 local iterations per communication round, and every communication round corresponds to an epoch, i.e. we use 300 global batch size for MNIST and 750 for CIFAR-10. For all datasets and methods, we use SGD with a constant learning rate of 0.01 after individually tuning in the set $\{0.5, 0.1, 0.05, 0.01, 0.005, 0.001\}$ and momentum coefficient of 0.9. For our method, we choose $\eta_2 = 0.01, \eta_3 = 0.001$ and use SGD without momentum. For synthetic, MNIST, and Fashion MNIST datasets we train for 150 epochs/comm. rounds and for CIFAR-10 for 250 epochs. We initialize $\sigma = 1$ in MNIST and Fashion MNIST experiments, and $\sigma = 0.4$ in synthetic experiments, and do not update σ for the first two epochs. For CIFAR-10 we initialize $\sigma = 0.2$ and we do lazy updates that is we start updates after 200 epochs. We observed lazy updates with relatively small initial σ works better for deeper models, whereas simpler models do not require it. To improve the empirical performance and have a more stable training we make a few changes to Algorithm 2. Namely, we keep individual σ for each scalar weight, for personalized and global models we clip the ℓ_∞ norm of the gradients by 1, and for σ by 10. We update σ at the first iteration instead of the last one. We include the global model in the local iterations.

Table 2: Total energy captured % averaged over samples and clients in the real dataset experiments.

Dataset	Method	Latent dimensionality	
		<i>Low</i>	<i>High</i>
<i>MNIST</i>	Baseline	78.9 ± 0.5	85.7 ± 0.4
	ADEPT-AE	70.8 ± 0.5	77.7 ± 0.1
	FedAvg	66.2 ± 0.9	75.9 ± 0.7
	Local Training	67.0 ± 0.8	69.1 ± 1.1
<i>F. MNIST</i>	Baseline	88.5 ± 0.2	91.3 ± 0.1
	ADEPT-AE	83.9 ± 0.2	85.6 ± 0.2
	FedAvg	81.2 ± 0.2	84.9 ± 0.2
	Local Training	76.9 ± 2.0	77.1 ± 0.5
<i>CIFAR-10</i>	Baseline	88.7 ± 0.5	93.3 ± 0.1
	ADEPT-AE	88.4 ± 0.5	93.3 ± 0.2
	FedAvg	87.4 ± 0.2	91.2 ± 0.1
	Local Training	87.7 ± 0.2	92.2 ± 0.2

ADEPT-DGM: For diffusion experiments we use a 6-layer U-Net from Hugging Face. We let every client to have access to 1200 or 600 samples from one class depending on the experiment. Instead of FedAvg, we compare to FedAvg+fine-tuning, as FedAvg cannot exclusively generate samples from the client's target distribution.

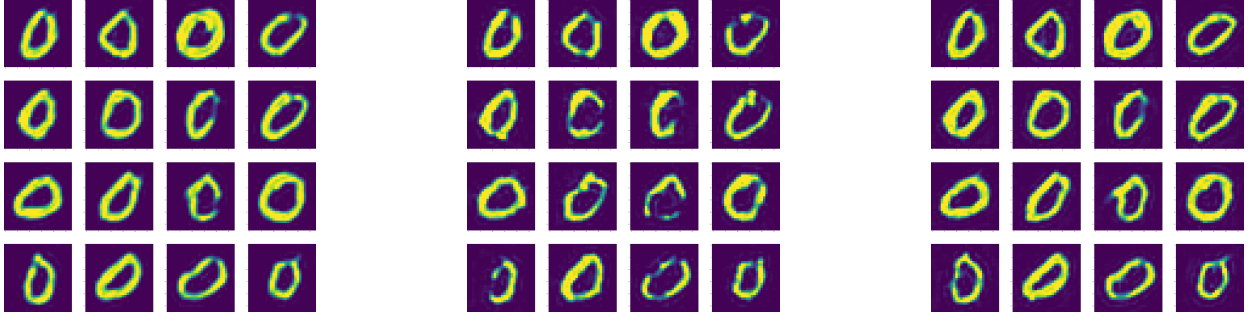


Figure 3: Randomly chosen samples (Left:ADEPT-DGM, noise $\sigma = 0.024$; Middle:FedAvg+fine-tuning,noise $\sigma = 0.028$; Right:Local training, noise $\sigma = 0.032$) (models are trained and samples are chosen with the same seed across runs) from generated dataset for a client with data from '0' class.

Training and hyper-parameters. We train using 20 local iterations per communication round and epoch. We use Adam optimizer with $1e-3$ for all methods. For our method, we use Adam with 0.01 learning rate for the updates of the global model and SGD with 0.001 lr for σ . We do 100 epochs/comm. rounds in total. We initialize $\sigma = 0.8$ and do not update for the first 2 epochs. We multiply the learning rates η_1, η_2 by 0.1 at 75th epoch. We employ the same changes in Algorithm 2 in Algorithm 3 as well. For a simpler demonstration, we use a variance preserving SDE (as in Algorithm 3) instead of variance exploding (as in Section 4). We do the same to modify Algorithm 3 as we did for ADEPT-DGM.

5.2 Results

Table 3: Diffusion model generation quality for generating MNIST samples using U-Net model (lower is better).

Method	Metric	
	<i>FID</i>	<i>KID</i>
Baseline	72.3 ± 2.2	0.062 ± 0.003
<i>High Number of Samples</i>		
ADEPT-DGM	80.0 ± 2.3	0.067 ± 0.003
FedAvg+fine-tuning	88.5 ± 3.8	0.082 ± 0.004
Local Training	84.1 ± 0.8	0.075 ± 0.001
<i>Low Number of Samples</i>		
ADEPT-DGM	84.2 ± 1.5	0.069 ± 0.002
FedAvg+fine-tuning	95.9 ± 7.6	0.090 ± 0.009
Local Training	91.8 ± 2.0	0.083 ± 0.003

ADEPT-PCA: We compare the reconstruction error between Algorithm 1, local training, and global training. In the global training setting, we train a single global model with the average of local gradients in each iteration. In Figure 2, the value in the y -axis is the ratio of the reconstruction error of each training method to the true error, which is evaluated by $\{U_i^*\}_{i=1}^m$. When σ^* is small, the heterogeneity of the data among the clients is low, and thus global training benefits from the sample size and performs better than pure local training. Our algorithm also makes use of the sample size and achieves an even smaller reconstruction error with the personalized models. When σ^* is large, the heterogeneity of the data among the clients is high and thus training a single global model for each client does not work well. In this case, our algorithm learns a

larger σ and performs more like local training. In the scenario between the two cases, our algorithm also outperforms both global and local training.

ADEPT-AE: The results are in terms of percentage of total energy captured per sample which is, for a sample x , equal to $100(1 - \|x - \hat{x}\|^2/\|x\|^2)$. The results are averaged over 3 runs and reported together with the standard deviation.

Synthetic data. In Table 1, baseline denotes that each client trains a personalized AE whose decoder part is the true data generating decoder. Our method outperforms local and global training and even the competitive baseline when heterogeneity is smaller. The result is similar to Figure 2, showing our method outperforms both local and global training in the regimes where they are strong alternatives.

Real data. The competitive baseline in (Table 2) is when 10 clients maintain all the training data from their corresponding class ($n = 5000$ per client). Remarkably, our method ($n = 250$ per client) matches the baseline on CIFAR-10 (for high latent dimensions), indicating that adaptive personalized collaboration results in $\times 20$ effective sample size. For other datasets, our method consistently outperforms FedAvg and local training by an important margin regardless of latent dimensionality. Our method reduces reconstruction error by as much as $\sim 35\%$ and $\sim 25\%$ compared to local training and FedAvg respectively.

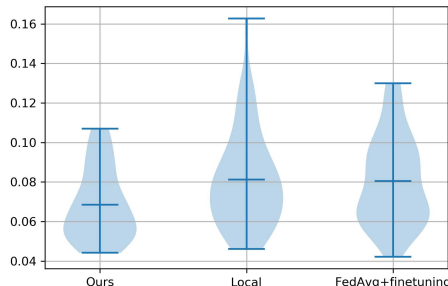


Figure 4: Violin plot of KID values of clients.

ADEPT-DGM: For Diffusion models we use FID [14] and KID [2] metrics to quantitatively measure the generated dataset quality (see Table 3). At the end of training, each client generates 200 samples (using the model with the lowest validation loss) and compares it to the local test dataset to compute the metrics. Our method consistently results in better quality generated samples and improves upon other methods by 5% – 22%. Moreover, in Figure 4 we depict the resulting KID values of clients. We see that our method brings equity, that is, the worst-performing client is much better compared to the worst clients of other methods; and the performance variance of clients is lower. We also illustrate randomly chosen sample images in Figure 3 and estimate the amount of noise using [15]. Compared to ADEPT-DGM, in images obtained using FedAvg+fine-tuning we observe missing features and inconsistent hallucinations. On the other hand, local training outputs images with significantly more background noise as apparent in images (e.g. 1st from the last row and 2nd from the first row) and from the estimated noise standard deviation which indicates a $1.5\times$ increase in noise level in terms of noise standard deviation ($\sigma = 0.032$ for local training vs $\sigma = 0.024$ for adaptive personalized method).

6 Conclusion

We developed, ADEPT, a hierarchical Bayes framework for personalized federated unsupervised learning; leading to new criteria for linear (ADEPT-PCA), non-linear (ADEPT-AE) dimensionality reduction, and personalized federated diffusion models (ADEPT-DGM). Each of our algorithms included adaptation for the heterogeneity during training which resulted in novel theoretical interpretations and superior empirical performance. Open questions include extensions with information constraints such as communication and privacy.

References

- [1] Durmus Alp Emre Acar, Yue Zhao, Ruizhao Zhu, Ramon Matas, Matthew Mattina, Paul Whatmough, and Venkatesh Saligrama. Debiasing model updates for improving personalized federated training. In *International Conference on Machine Learning*, pages 21–31. PMLR, 2021.
- [2] Miłkołaj Bińkowski, Dougal J. Sutherland, Michael Arbel, and Arthur Gretton. Demystifying MMD GANs. In *International Conference on Learning Representations*, 2018.
- [3] Xingjian Cao, Gang Sun, Hongfang Yu, and Mohsen Guizani. Perfed-gan: Personalized federated learning via generative adversarial networks. *IEEE Internet of Things Journal*, 10(5):3749–3762, 2023.
- [4] Huili Chen, Jie Ding, Eric William Tramel, Shuang Wu, Anit Kumar Sahu, Salman Avestimehr, and Tao Zhang. Self-aware personalized federated learning. In Alice H. Oh, Alekh Agarwal, Danielle Belgrave, and Kyunghyun Cho, editors, *Advances in Neural Information Processing Systems*, 2022.
- [5] Shixiang Chen, Alfredo Garcia, Mingyi Hong, and Shahin Shahrampour. Decentralized riemannian gradient descent on the stiefel manifold. In *International Conference on Machine Learning*, pages 1594–1605. PMLR, 2021.
- [6] Liam Collins, Hamed Hassani, Aryan Mokhtari, and Sanjay Shakkottai. Exploiting shared representations for personalized federated learning. In Marina Meila and Tong Zhang, editors, *International Conference on Machine Learning (ICML)*, volume 139 of *Proceedings of Machine Learning Research*, pages 2089–2099. PMLR, 2021.
- [7] Yuyang Deng, Mohammad Mahdi Kamani, and Mehrdad Mahdavi. Adaptive personalized federated learning. *arXiv preprint arXiv:2003.13461*, 2020.
- [8] Canh T. Dinh, Nguyen H. Tran, and Tuan Dung Nguyen. Personalized federated learning with moreau envelopes. In *Advances in Neural Information Processing Systems*, 2020.
- [9] Simon Shaolei Du, Wei Hu, Sham M. Kakade, Jason D. Lee, and Qi Lei. Few-shot learning via learning the representation, provably. In *International Conference on Learning Representations*, 2021.
- [10] Bradley Efron. *Large-Scale Inference: Empirical Bayes Methods for Estimation, Testing, and Prediction*. Institute of Mathematical Statistics Monographs. Cambridge University Press, 2010.
- [11] Alireza Fallah, Aryan Mokhtari, and Asuman Ozdaglar. Personalized federated learning: A meta-learning approach. In *Advances in Neural Information Processing Systems*, 2020.
- [12] Avishek Ghosh, Jichan Chung, Dong Yin, and Kannan Ramchandran. An efficient framework for clustered federated learning. In *Advances in Neural Information Processing Systems*, 2020.
- [13] Filip Hanzely and Peter Richtárik. Federated learning of a mixture of global and local models. *arXiv preprint arXiv:2002.05516*, 2020.
- [14] Martin Heusel, Hubert Ramsauer, Thomas Unterthiner, Bernhard Nessler, and Sepp Hochreiter. Gans trained by a two time-scale update rule converge to a local nash equilibrium. *Advances in neural information processing systems*, 30, 2017.
- [15] John Immerkær. Fast noise variance estimation. *Computer Vision and Image Understanding*, 64(2):300–302, 1996.
- [16] Peter Kairouz, H Brendan McMahan, Brendan Avent, Aurélien Bellet, Mehdi Bennis, Arjun Nitin Bhagoji, Kallista Bonawitz, Zachary Charles, Graham Cormode, Rachel Cummings, et al. Advances and open problems in federated learning. *Foundations and Trends® in Machine Learning*, 14(1–2):1–210, 2021.
- [17] Mikhail Khodak, Maria-Florina F Balcan, and Ameet S Talwalkar. Adaptive gradient-based meta-learning methods. In *Advances in Neural Information Processing Systems*, 2019.

- [18] Diederik P Kingma and Ruiqi Gao. Understanding diffusion objectives as the ELBO with simple data augmentation. In *Thirty-seventh Conference on Neural Information Processing Systems*, 2023.
- [19] Diederik P Kingma, Tim Salimans, Ben Poole, and Jonathan Ho. On density estimation with diffusion models. In A. Beygelzimer, Y. Dauphin, P. Liang, and J. Wortman Vaughan, editors, *Advances in Neural Information Processing Systems*, 2021.
- [20] Nikita Yurevich Kotelevskii, Maxime Vono, Alain Durmus, and Eric Moulines. Fedpop: A bayesian approach for personalised federated learning. In Alice H. Oh, Alekh Agarwal, Danielle Belgrave, and Kyunghyun Cho, editors, *Advances in Neural Information Processing Systems*, 2022.
- [21] Qi Le, Enmao Diao, Xinran Wang, Ali Anwar, Vahid Tarokh, and Jie Ding. Personalized federated recommender systems with private and partially federated autoencoders, 2022.
- [22] Tian Li, Anit Kumar Sahu, Manzil Zaheer, Maziar Sanjabi, Ameet Talwalkar, and Virginia Smith. Federated optimization in heterogeneous networks. In *Proceedings of Machine Learning and Systems 2020, MLSys*, 2020.
- [23] Jian Ma, Junhao Liang, Chen Chen, and Haonan Lu. Subject-diffusion: Open domain personalized text-to-image generation without test-time fine-tuning. *arXiv preprint arXiv:2307.11410*, 2023.
- [24] Yishay Mansour, Mehryar Mohri, Jae Ro, and Ananda Theertha Suresh. Three approaches for personalization with applications to federated learning. *arXiv preprint arXiv:2002.10619*, 2020.
- [25] Othmane Marfoq, Giovanni Neglia, Aurélien Bellet, Laetitia Kamani, and Richard Vidal. Federated multi-task learning under a mixture of distributions. *Advances in Neural Information Processing Systems*, 34, 2021.
- [26] Brendan McMahan, Eider Moore, Daniel Ramage, Seth Hampson, and Blaise Agueria y Arcas. Communication-efficient learning of deep networks from decentralized data. In *Artificial Intelligence and Statistics*, pages 1273–1282. PMLR, 2017.
- [27] Taehong Moon, Moonseok Choi, Gayoung Lee, Jung-Woo Ha, and Juho Lee. Fine-tuning diffusion models with limited data. In *NeurIPS 2022 Workshop on Score-Based Methods*, 2022.
- [28] Kaan Ozkara, Antonious Girgis, Deepesh Data, and Suhas Diggavi. A statistical framework for personalized federated learning and estimation: Theory, algorithms, and privacy. In *International Conference on Learning Representations*, 2023.
- [29] Kaan Ozkara, Bruce Huang, and Suhas Diggavi. Personalized PCA for federated heterogeneous data. In *2023 IEEE International Symposium on Information Theory (ISIT)*, pages 168–173. IEEE, 2023.
- [30] Kaan Ozkara, Navjot Singh, Deepesh Data, and Suhas Diggavi. Quped: Quantized personalization via distillation with applications to federated learning. *Advances in Neural Information Processing Systems*, 34, 2021.
- [31] Chao Peng, Yiming Guo, Yao Chen, Qilin Rui, Zhengfeng Yang, and Chenyang Xu. Fedgm: Heterogeneous federated learning via generative learning and mutual distillation. In *Euro-Par 2023: Parallel Processing: 29th International Conference on Parallel and Distributed Computing, Limassol, Cyprus, August 28 – September 1, 2023, Proceedings*, page 339–351, Berlin, Heidelberg, 2023. Springer-Verlag.
- [32] Mirko Polato. Federated variational autoencoder for collaborative filtering. In *2021 International Joint Conference on Neural Networks (IJCNN)*, pages 1–8, 2021.
- [33] Danilo Rezende and Shakir Mohamed. Variational inference with normalizing flows. In *International conference on machine learning*, pages 1530–1538. PMLR, 2015.
- [34] Nataniel Ruiz, Yuanzhen Li, Varun Jampani, Yael Pritch, Michael Rubinstein, and Kfir Aberman. Dreambooth: Fine tuning text-to-image diffusion models for subject-driven generation. In *Proceedings of the IEEE/CVF Conference on Computer Vision and Pattern Recognition*, pages 22500–22510, 2023.

- [35] Naichen Shi and Raed Al Kontar. Personalized PCA: Decoupling shared and unique features. *arXiv preprint arXiv:2207.08041*, 2022.
- [36] Virginia Smith, Chao-Kai Chiang, Maziar Sanjabi, and Ameet S. Talwalkar. Federated multi-task learning. In *Advances in Neural Information Processing Systems*, pages 4424–4434, 2017.
- [37] Jascha Sohl-Dickstein, Eric A. Weiss, Niru Maheswaranathan, and Surya Ganguli. Deep unsupervised learning using nonequilibrium thermodynamics. In *Proceedings of the 32nd International Conference on Machine Learning, ICML 2015, Lille, France, 6-11 July 2015*, volume 37 of *JMLR Workshop and Conference Proceedings*, pages 2256–2265. JMLR.org, 2015.
- [38] Jiaming Song, Chenlin Meng, and Stefano Ermon. Denoising diffusion implicit models. In *International Conference on Learning Representations*, 2021.
- [39] Yang Song, Jascha Sohl-Dickstein, Diederik P Kingma, Abhishek Kumar, Stefano Ermon, and Ben Poole. Score-based generative modeling through stochastic differential equations. In *International Conference on Learning Representations*, 2021.
- [40] Yonglong Tian, Yue Wang, Dilip Krishnan, Joshua B Tenenbaum, and Phillip Isola. Rethinking few-shot image classification: a good embedding is all you need? In *European Conference on Computer Vision*, pages 266–282. Springer, 2020.
- [41] Michael E Tipping and Christopher M Bishop. Probabilistic principal component analysis. *Journal of the Royal Statistical Society: Series B (Statistical Methodology)*, 61(3):611–622, 1999.
- [42] Ye Lin Tun, Chu Myaet Thwal, Ji Su Yoon, Sun Moo Kang, Chaoning Zhang, and Choong Seon Hong. Federated learning with diffusion models for privacy-sensitive vision tasks. In *2023 International Conference on Advanced Technologies for Communications (ATC)*, pages 305–310. IEEE, 2023.
- [43] Paul Vanhaesebrouck, Aurélien Bellet, and Marc Tommasi. Decentralized collaborative learning of personalized models over networks. In *Artificial Intelligence and Statistics*, pages 509–517. PMLR, 2017.
- [44] Lei Yang, Jiaming Huang, Wanyu Lin, and Jiannong Cao. Personalized federated learning on non-iid data via group-based meta-learning. *ACM Transactions on Knowledge Discovery from Data*, 17(4):1–20, 2023.
- [45] Valentina Zantedeschi, Aurélien Bellet, and Marc Tommasi. Fully decentralized joint learning of personalized models and collaboration graphs. In *International Conference on Artificial Intelligence and Statistics*, pages 864–874. PMLR, 2020.
- [46] Lvmin Zhang, Anyi Rao, and Maneesh Agrawala. Adding conditional control to text-to-image diffusion models. In *Proceedings of the IEEE/CVF International Conference on Computer Vision*, pages 3836–3847, 2023.
- [47] Michael Zhang, Karan Sapra, Sanja Fidler, Serena Yeung, and Jose M. Alvarez. Personalized federated learning with first order model optimization. In *International Conference on Learning Representations*, 2021.

Appendix

A Proofs for Adaptive PCA: ADEPT-PCA

Theorem A.1. *By choosing $\eta_1 = \min\{\frac{1}{3C\eta_1}, 1\}$, $\eta_2 = \min\{\frac{1}{3C\eta_2}, 1\}$, and $\eta_3 = \min\{\frac{\eta_1}{3(L_U^{(\sigma)})^2}, \frac{\eta_2}{3(L_V^{(\sigma)})^2}, \frac{1}{bL_\sigma}\}$, we have*

$$\sum_{t=1}^T \left(\left(\frac{1}{m} \sum_{i=1}^m \|\mathbf{g}_{i,t}^U\|_F^2 \right) + \|\mathbf{g}_t^V\|_F^2 + (\mathbf{g}_t^\sigma)^2 \right) \leq \frac{3\Delta_T}{\min\{\eta_1, \eta_2, \eta_3\}}$$

where

$$\begin{aligned}
\mathbf{g}_t^{\mathbf{V}} &= P_{\mathcal{T}_{\mathbf{V}_{t-1}}} (\nabla_{\mathbf{V}_{t-1}} f^{\text{pca}}(\{\mathbf{U}_{i,t}\}_i, \mathbf{V}_{t-1}, \sigma_{t-1})), \\
\mathbf{g}_{i,t}^{\mathbf{U}} &= P_{\mathcal{T}_{\mathbf{U}_{i,t-1}}} (\nabla_{\mathbf{U}_{i,t-1}} f_i^{\text{pca}}(\mathbf{U}_{i,t-1}, \mathbf{V}_{t-1}, \sigma_{t-1})), \\
\mathbf{g}_t^{\sigma} &= \frac{\partial}{\partial \sigma_{t-1}} f^{\text{pca}}(\{\mathbf{U}_{i,t-1}\}_i, \mathbf{V}_{t-1}, \sigma_{t-1}), \\
\Delta_T &= f^{\text{pca}}(\{\mathbf{U}_{i,0}\}_i, \mathbf{V}_0, \sigma_0) - f^{\text{pca}}(\{\mathbf{U}_{i,T}\}_i, \mathbf{V}_T, \sigma_T).
\end{aligned}$$

A.1 Proofs

Fact A.2. The gradients of the local loss function with respect to the local and global PC's and σ are given as

$$\begin{aligned}
\nabla_{\mathbf{U}_i} f_i^{\text{pca}}(\mathbf{U}_i, \mathbf{V}, \sigma) &= -\frac{n}{2} (\mathbf{W}_i^{-1} \mathbf{S}_i \mathbf{W}_i^{-1} \mathbf{U}_i - \mathbf{W}_i^{-1} \mathbf{U}_i) + \frac{\mathcal{P}_{\mathcal{T}_{\mathbf{V}}}(\mathbf{U}_i)}{\sigma^2}, \\
\nabla_{\mathbf{V}} f_i^{\text{pca}}(\mathbf{U}_i, \mathbf{V}) &= -\frac{\mathcal{P}_{\mathcal{T}_{\mathbf{V}}}(\mathbf{U}_i) (\mathbf{U}_i^{\top} \mathbf{V} + \mathbf{V}^{\top} \mathbf{U}_i)}{2\sigma^2}, \\
\frac{\partial}{\partial \sigma} f_i^{\text{pca}}(\mathbf{U}_i, \mathbf{V}, \sigma) &= \frac{d}{\sigma} - \frac{2\xi + d^2(\mathbf{V}, \mathbf{U}_i)}{\sigma^3}, \\
\nabla_{\mathbf{U}_i} \left(\frac{\partial}{\partial \sigma} f_i^{\text{pca}}(\mathbf{U}_i, \mathbf{V}, \sigma) \right) &= -\frac{2\mathcal{P}_{\mathcal{T}_{\mathbf{V}}}(\mathbf{U}_i)}{\sigma^3}, \\
\nabla_{\mathbf{V}} \left(\frac{\partial}{\partial \sigma} f_i^{\text{pca}}(\mathbf{U}_i, \mathbf{V}, \sigma) \right) &= \frac{\mathcal{P}_{\mathcal{T}_{\mathbf{V}}}(\mathbf{U}_i) (\mathbf{U}_i^{\top} \mathbf{V} + \mathbf{V}^{\top} \mathbf{U}_i)}{\sigma^3}.
\end{aligned}$$

Fact A.3. For two matrices $\mathbf{A} \in \mathbb{R}^{a \times b}$ and $\mathbf{B} \in \mathbb{R}^{b \times c}$, we have

$$\|\mathbf{AB}\|_F \leq \|\mathbf{A}\|_{op} \|\mathbf{B}\|_F \text{ and } \|\mathbf{AB}\|_F \leq \|\mathbf{A}\|_F \|\mathbf{B}\|_{op}.$$

Fact A.4. For matrix to matrix functions, $\{g_i\}_{i=1}^k$, with bounded output operator norms, $\max_{\mathbf{X}} \|g_i(\mathbf{X})\|_{op} \leq M_i$, we have

$$\left\| \prod_{i=1}^k g_i(\mathbf{X}) - \prod_{i=1}^k g_i(\mathbf{Y}) \right\|_F \leq \prod_{j=1}^k M_j \left(\sum_{i=1}^k \|g_i(\mathbf{X}) - g_i(\mathbf{Y})\|_F \right)$$

A.1.1 Proof of Lemma 3.2

Proof. We use mathematical induction to proof the lemma. For the base case, it is given that $\sigma_0 \geq \omega \sqrt{\frac{2\xi}{d}}$. Assume that for all $\tau \in \{0, 1, \dots, t\}$,

$$\sigma_{\tau} \geq \omega \sqrt{\frac{2\xi}{d}}.$$

Then, we consider the following two cases. First, if $\sigma_t \in \left[\omega \sqrt{\frac{2\xi}{d}}, \sqrt{\frac{2\xi}{d}} \right]$, we have

$$\begin{aligned}
\sigma_t \leq \sqrt{\frac{2\xi}{d}} &\Rightarrow d \leq \frac{2\xi}{\sigma_t^2} \Rightarrow \frac{d}{\sigma_t} - \frac{2\xi}{\sigma_t^3} \leq 0 \\
\Rightarrow \forall i \in [m] : \frac{\partial}{\partial \sigma_t} f_i^{\text{pca}}(\mathbf{U}_{i,t}, \mathbf{V}_t, \sigma_t) &= \frac{d}{\sigma_t} - \frac{2\xi + d^2(\mathbf{V}_t, \mathbf{U}_{i,t})}{\sigma_t^3} \leq \frac{d}{\sigma_t} - \frac{2\xi}{\sigma_t^3} \leq 0 \\
\Rightarrow \forall i \in [m] : \sigma_{i,t+1} = \sigma_t - \eta_3 \frac{\partial}{\partial \sigma_t} f_i^{\text{pca}}(\mathbf{U}_{i,t}, \mathbf{V}_t, \sigma_t) &\geq \sigma_t \geq \omega \sqrt{\frac{2\xi}{d}} \\
\Rightarrow \sigma_{t+1} = \frac{1}{m} \sum_{i=1}^m \sigma_{i,t+1} &\geq \omega \sqrt{\frac{2\xi}{d}}.
\end{aligned}$$

Otherwise, if we have $\sigma_t > \sqrt{\frac{2\xi}{d}}$, we have

$$\begin{aligned}\sigma_{i,t+1} &= \sigma_t - \eta_3 \frac{\partial}{\partial \sigma_t} f_i^{\text{pca}}(\mathbf{U}_{i,t}, \mathbf{V}_t, \sigma_t) = \sigma_t - \eta_3 \left(\frac{d}{\sigma_t} - \frac{2\xi + d^2(\mathbf{V}_t, \mathbf{U}_{i,t})}{\sigma_t^3} \right) \\ &\geq \sigma_t - \eta_3 \frac{d}{\sigma_t} \geq \sqrt{\frac{2\xi}{d}} - (1-\omega) \frac{2\xi}{d^2} \cdot \frac{d}{\sqrt{2\xi/d}} = \omega \sqrt{\frac{2\xi}{d}}\end{aligned}$$

and thus

$$\sigma_{t+1} = \frac{1}{m} \sum_{i=1}^m \sigma_{i,t+1} \geq \omega \sqrt{\frac{2\xi}{d}}.$$

Thus, by mathematical induction, we have

$$\forall t \in \mathbb{N} \quad \forall i \in [m] : \quad \sigma_t \geq \omega \sqrt{\frac{2\xi}{d}} \quad \text{and} \quad \sigma_{i,t} \geq \omega \sqrt{\frac{2\xi}{d}}.$$

□

A.1.2 Proof of Lemma 3.6

Proof. For the Lipschitz smoothness, we have

$$\begin{aligned}\left| \frac{\partial^2}{\partial \sigma^2} f_i^{\text{pca}}(\mathbf{U}_i, \mathbf{V}, \sigma) \right| &= \left| \frac{6\xi + 3d^2(\mathbf{V}, \mathbf{U}_i)}{\sigma^4} - \frac{d}{\sigma^2} \right| \\ &\leq \left| \frac{6\xi + 3d^2(\mathbf{V}, \mathbf{U}_i)}{\sigma^4} \right| + \left| \frac{d}{\sigma^2} \right| \\ &\leq \frac{6\xi + 12}{4\xi^2\omega^4/d^2} + \frac{d}{2\xi\omega^2/d} \\ &= \frac{3d^2}{2\xi\omega^4} + \frac{3d^2}{\xi^2\omega^4} + \frac{d^2}{2\xi\omega^2} \\ &= L_\sigma\end{aligned}$$

for any \mathbf{V}, \mathbf{U}_i , and $\sigma \geq \omega \sqrt{\frac{2\xi}{d}}$.

□

A.1.3 Proof of Lemma 3.7

Proof. For the bound on the gradient,

$$\begin{aligned}&\left\| -\frac{n}{2}(\mathbf{W}_i^{-1}S_i\mathbf{W}_i^{-1}\mathbf{U}_i - \mathbf{W}_i^{-1}\mathbf{U}_i) + \frac{\mathcal{P}\mathcal{T}_{\mathbf{V}}(\mathbf{U}_i)}{\sigma^2} \right\|_{op} \\ &\leq \left\| -\frac{n}{2}(\mathbf{W}_i^{-1}S_i\mathbf{W}_i^{-1}\mathbf{U}_i - \mathbf{W}_i^{-1}\mathbf{U}_i) \right\|_{op} + \frac{2}{\sigma^2} \\ &\leq \frac{n}{2}(\|\mathbf{W}_i^{-1}S_i\mathbf{W}_i^{-1}\mathbf{U}_i\|_{op} + \|\mathbf{W}_i^{-1}\mathbf{U}_i\|_{op}) + \frac{2}{\sigma^2} \\ &\leq \frac{n}{2} \left(\frac{G_{max,op}}{\sigma_\epsilon^4} + \frac{1}{\sigma_\epsilon^2} \right) + \frac{d}{\xi\omega^2},\end{aligned}$$

where in the last inequality we use $\|\mathbf{W}_i^{-1}\|_{op} \leq \frac{1}{\sigma_\epsilon^2}$. Therefore, we find that norm of the gradient is bounded by $G_U := \frac{n}{2} \left(\frac{G_{max,op}}{\sigma_\epsilon^4} + \frac{1}{\sigma_\epsilon^2} \right) + \frac{d}{\xi\omega^2}$. For the Lipschitz continuity of the gradient, we omit the client index i and use \mathbf{U}_1 and \mathbf{U}_2 to denote two arbitrary points on $St(d, r)$ for simplicity. For any client i , we focus on the first term of the gradient,

$$\|\mathbf{W}_1^{-1}S_i\mathbf{W}_1^{-1}\mathbf{U}_1 - \mathbf{W}_1^{-1}\mathbf{U}_1 - \mathbf{W}_2^{-1}S_i\mathbf{W}_2^{-1}\mathbf{U}_2 + \mathbf{W}_2^{-1}\mathbf{U}_2\|_F$$

$$\leq \left(\frac{1}{\sigma_\epsilon^2} + \frac{G_{max,op}}{\sigma_\epsilon^4} + \left(1 + \frac{2G_{max,op}}{\sigma_\epsilon^2} \right) \frac{2}{\sigma_\epsilon^4} \right) \|\mathbf{U}_2 - \mathbf{U}_1\|_F, \quad (17)$$

For the second part of the gradient we have

$$\begin{aligned} & \frac{1}{\sigma^2} \|\mathcal{P}_{\mathcal{T}_V}(\mathbf{U}_1) - \mathcal{P}_{\mathcal{T}_V}(\mathbf{U}_2)\|_F \\ &= \frac{1}{\sigma^2} \|\mathbf{U}_1 - \mathbf{U}_2 - \frac{1}{2} \mathbf{V}(\mathbf{V}^\top(\mathbf{U}_1 - \mathbf{U}_2) + (\mathbf{U}_1^\top - \mathbf{U}_2^\top)\mathbf{V})\|_F \\ &\leq \frac{2}{\sigma^2} \|\mathbf{U}_1 - \mathbf{U}_2\|_F, \\ &\leq \frac{d}{\xi\omega^2} \|\mathbf{U}_1 - \mathbf{U}_2\|_F, \end{aligned}$$

where in the last inequality we use Fact A.3. As a result, we find that the gradient is Lipschitz continuous with $L_U := \frac{n}{2} \left(\frac{1}{\sigma_\epsilon^2} + \frac{G_{max,op}}{\sigma_\epsilon^4} + \left(1 + \frac{2G_{max,op}}{\sigma_\epsilon^2} \right) \frac{2}{\sigma_\epsilon^4} \right) + \frac{d}{\xi\omega^2}$. \square

A.1.4 Proof of Lemma 3.8

Proof. For the Lipschitz constant

$$\begin{aligned} & \frac{2}{\sigma^2} \|\mathcal{P}_{\mathcal{T}_{V_1}}(\mathbf{U}_i) \text{sym}(\mathbf{U}_i^\top \mathbf{V}_1) - \mathcal{P}_{\mathcal{T}_{V_2}}(\mathbf{U}_i) \text{sym}(\mathbf{U}_i^\top \mathbf{V}_2)\|_F \\ &= \frac{2}{\sigma^2} \|\mathbf{U}_i \mathbf{U}_i^\top (\mathbf{V}_1 - \mathbf{V}_2) + \mathbf{U}_i (\mathbf{V}_1 - \mathbf{V}_2) \mathbf{U}_i^\top - \frac{1}{2} (\mathbf{V}_1 (\mathbf{V}_1^\top \mathbf{U}_i + \mathbf{U}_i^\top \mathbf{V}_1) - \mathbf{V}_2 (\mathbf{V}_2^\top \mathbf{U}_i + \mathbf{U}_i^\top \mathbf{V}_2))\|_F \\ &\leq \frac{24}{\sigma^2} \|\mathbf{V}_1 - \mathbf{V}_2\|_F \\ &\leq \frac{12d}{\xi\omega^2}, \end{aligned}$$

where $\text{sym}(\mathbf{U}_i^\top \mathbf{V}) = \mathbf{U}_i^\top \mathbf{V} + \mathbf{V}^\top \mathbf{U}_i$ and we used Fact A.4, hence $L_V = \frac{12d}{\xi\omega^2}$. For the gradient bound, it is straightforward to see that

$$\|\nabla_{\mathbf{V}} f_i^{\text{pca}}(\mathbf{U}, \mathbf{V}, \sigma)\|_2 \leq \frac{4}{\sigma^2} \leq \frac{2d}{\xi\omega^2}.$$

\square

A.1.5 Proof of Lemma 3.9

Proof. Using Fact A.2, we have

$$\|\nabla_{\mathbf{U}_i} \left(\frac{\partial}{\partial \sigma} f_i^{\text{pca}}(\mathbf{U}_i, \mathbf{V}, \sigma) \right)\|_2 \leq \frac{4}{\sigma^3} \leq \frac{\sqrt{2d^3}}{\omega^3 \sqrt{\xi^3}}$$

and

$$\|\nabla_{\mathbf{V}} \left(\frac{\partial}{\partial \sigma} f_i^{\text{pca}}(\mathbf{U}_i, \mathbf{V}, \sigma) \right)\|_2 \leq \frac{8}{\sigma^3} \leq \frac{2\sqrt{2d^3}}{\omega^3 \sqrt{\xi^3}}$$

\square

A.1.6 Proof of Lemma 3.10

Proof. We have

$$f^{\text{pca}}(\{\mathbf{U}_{i,t}\}_i, \mathbf{V}_t, \sigma_t) - f^{\text{pca}}(\{\mathbf{U}_{i,t-1}\}_i, \mathbf{V}_{t-1}, \sigma_{t-1})$$

$$\begin{aligned}
&= [f^{\text{pca}}(\{\mathbf{U}_{i,t}\}_i, \mathbf{V}_t, \sigma_t) - f^{\text{pca}}(\{\mathbf{U}_{i,t}\}_i, \mathbf{V}_t, \sigma_{t-1})] \\
&+ [f^{\text{pca}}(\{\mathbf{U}_{i,t}\}_i, \mathbf{V}_t, \sigma_{t-1}) - f^{\text{pca}}(\{\mathbf{U}_{i,t}\}_i, \mathbf{V}_{t-1}, \sigma_{t-1})] \\
&+ [f^{\text{pca}}(\{\mathbf{U}_{i,t}\}_i, \mathbf{V}_{t-1}, \sigma_{t-1}) - f^{\text{pca}}(\{\mathbf{U}_{i,t-1}\}_i, \mathbf{V}_{t-1}, \sigma_{t-1})]
\end{aligned}$$

With a similar proof as Lemma 5 in [29], we have

$$\begin{aligned}
&f^{\text{pca}}(\{\mathbf{U}_{i,t}\}_i, \mathbf{V}_{t-1}, \sigma_{t-1}) - f^{\text{pca}}(\{\mathbf{U}_{i,t-1}\}_i, \mathbf{V}_{t-1}, \sigma_{t-1}) \\
&\leq \frac{(-\eta_1 + C\eta_1\eta_1^2)}{m} \sum_{i=1}^m \|P_{\mathcal{T}_{\mathbf{U}_{i,t-1}}}(\nabla_{\mathbf{U}_{i,t-1}} f_i^{\text{pca}}(\mathbf{U}_{i,t-1}, \mathbf{V}_{t-1}, \sigma_{t-1}))\|_F^2, \\
&f^{\text{pca}}(\{\mathbf{U}_{i,t}\}_i, \mathbf{V}_t, \sigma_{t-1}) - f^{\text{pca}}(\{\mathbf{U}_{i,t}\}_i, \mathbf{V}_{t-1}, \sigma_{t-1}) \\
&\leq (-\eta_2 + C\eta_2\eta_2^2) \|P_{\mathcal{T}_{\mathbf{V}_{t-1}}}(\nabla_{\mathbf{V}_{t-1}} f^{\text{pca}}(\{\mathbf{U}_{i,t}\}_i, \mathbf{V}_{t-1}, \sigma_{t-1}))\|_F^2
\end{aligned}$$

where

$$\begin{aligned}
C\eta_1 &= C_1 G_1 + \frac{L_{gu}(C_1^2 G_1^2 + 1)}{2}, \\
C\eta_2 &= C_2 G_2 + \frac{L_{gv}(C_2^2 G_2^2 + 1)}{2}, \\
G_1 &= 2G_U \sqrt{d}, \\
G_2 &= 2G_V \sqrt{d}
\end{aligned}$$

with some constants C_1, C_2 given by Lemma 3.4 and G_U, G_V given in Lemma 3.7, 3.8. For the sufficient decrease with respect to σ , we have

$$\begin{aligned}
&f^{\text{pca}}(\{\mathbf{U}_{i,t}\}_i, \mathbf{V}_t, \sigma_t) - f^{\text{pca}}(\{\mathbf{U}_{i,t}\}_i, \mathbf{V}_t, \sigma_{t-1}) \\
&\leq \frac{\partial}{\partial \sigma_{t-1}} f^{\text{pca}}(\{\mathbf{U}_{i,t}\}_i, \mathbf{V}_t, \sigma_{t-1})(\sigma_t - \sigma_{t-1}) + \frac{L_\sigma}{2}(\sigma_t - \sigma_{t-1})^2 \\
&= \left[\frac{\partial}{\partial \sigma_{t-1}} f^{\text{pca}}(\{\mathbf{U}_{i,t}\}_i, \mathbf{V}_t, \sigma_{t-1}) \right] \left[-\eta_3 \frac{\partial}{\partial \sigma_{t-1}} f^{\text{pca}}(\{\mathbf{U}_{i,t-1}\}_i, \mathbf{V}_{t-1}, \sigma_{t-1}) \right] + \frac{\eta_3^2 L_\sigma}{2} \left[\frac{\partial}{\partial \sigma_{t-1}} f^{\text{pca}}(\{\mathbf{U}_{i,t-1}\}_i, \mathbf{V}_{t-1}, \sigma_{t-1}) \right]^2 \\
&\hspace{15em} \text{(by the update rule of } \sigma_t \text{)} \\
&= (-\eta_3) \left[\frac{\partial}{\partial \sigma_{t-1}} f^{\text{pca}}(\{\mathbf{U}_{i,t}\}_i, \mathbf{V}_t, \sigma_{t-1}) - \frac{\partial}{\partial \sigma_{t-1}} f^{\text{pca}}(\{\mathbf{U}_{i,t-1}\}_i, \mathbf{V}_{t-1}, \sigma_{t-1}) + \frac{\partial}{\partial \sigma_{t-1}} f^{\text{pca}}(\{\mathbf{U}_{i,t-1}\}_i, \mathbf{V}_{t-1}, \sigma_{t-1}) \right] \\
&\quad \cdot \left[\frac{\partial}{\partial \sigma_{t-1}} f^{\text{pca}}(\{\mathbf{U}_{i,t-1}\}_i, \mathbf{V}_{t-1}, \sigma_{t-1}) \right] + \frac{\eta_3^2 L_\sigma}{2} \left[\frac{\partial}{\partial \sigma_{t-1}} f^{\text{pca}}(\{\mathbf{U}_{i,t-1}\}_i, \mathbf{V}_{t-1}, \sigma_{t-1}) \right]^2 \\
&= (-\eta_3) \left[\frac{\partial}{\partial \sigma_{t-1}} f^{\text{pca}}(\{\mathbf{U}_{i,t}\}_i, \mathbf{V}_t, \sigma_{t-1}) - \frac{\partial}{\partial \sigma_{t-1}} f^{\text{pca}}(\{\mathbf{U}_{i,t-1}\}_i, \mathbf{V}_{t-1}, \sigma_{t-1}) \right] \left[\frac{\partial}{\partial \sigma_{t-1}} f^{\text{pca}}(\{\mathbf{U}_{i,t-1}\}_i, \mathbf{V}_{t-1}, \sigma_{t-1}) \right] \\
&\quad - \left(\eta_3 - \frac{\eta_3^2 L_\sigma}{2} \right) \left[\frac{\partial}{\partial \sigma_{t-1}} f^{\text{pca}}(\{\mathbf{U}_{i,t-1}\}_i, \mathbf{V}_{t-1}, \sigma_{t-1}) \right]^2 \\
&\leq \frac{\eta_3}{2} \left[\frac{\partial}{\partial \sigma_{t-1}} f^{\text{pca}}(\{\mathbf{U}_{i,t}\}_i, \mathbf{V}_t, \sigma_{t-1}) - \frac{\partial}{\partial \sigma_{t-1}} f^{\text{pca}}(\{\mathbf{U}_{i,t-1}\}_i, \mathbf{V}_{t-1}, \sigma_{t-1}) \right]^2 + \frac{\eta_3}{2} \left[\frac{\partial}{\partial \sigma_{t-1}} f^{\text{pca}}(\{\mathbf{U}_{i,t-1}\}_i, \mathbf{V}_{t-1}, \sigma_{t-1}) \right]^2 \\
&\quad - \left(\eta_3 - \frac{\eta_3^2 L_\sigma}{2} \right) \left[\frac{\partial}{\partial \sigma_{t-1}} f^{\text{pca}}(\{\mathbf{U}_{i,t-1}\}_i, \mathbf{V}_{t-1}, \sigma_{t-1}) \right]^2 \hspace{5em} \text{(since } 2ab \leq a^2 + b^2 \text{ for any } a, b \in \mathbb{R} \text{)} \\
&= \frac{\eta_3}{2} \left[\frac{\partial}{\partial \sigma_{t-1}} f^{\text{pca}}(\{\mathbf{U}_{i,t}\}_i, \mathbf{V}_t, \sigma_{t-1}) - \frac{\partial}{\partial \sigma_{t-1}} f^{\text{pca}}(\{\mathbf{U}_{i,t-1}\}_i, \mathbf{V}_{t-1}, \sigma_{t-1}) \right]^2 - \left(\frac{\eta_3}{2} - \frac{\eta_3^2 L_\sigma}{2} \right) \left[\frac{\partial}{\partial \sigma_{t-1}} f^{\text{pca}}(\{\mathbf{U}_{i,t-1}\}_i, \mathbf{V}_{t-1}, \sigma_{t-1}) \right]^2 \\
&= \frac{\eta_3}{2} \left[\frac{\partial}{\partial \sigma_{t-1}} f^{\text{pca}}(\{\mathbf{U}_{i,t}\}_i, \mathbf{V}_t, \sigma_{t-1}) - \frac{\partial}{\partial \sigma_{t-1}} f_i^{\text{pca}}(\mathbf{V}_t, \{\mathbf{U}_{i,t-1}\}_i, \sigma_{t-1}) \right. \\
&\quad \left. + \frac{\partial}{\partial \sigma_{t-1}} f^{\text{pca}}(\{\mathbf{U}_{i,t-1}\}_i, \mathbf{V}_t, \sigma_{t-1}) - \frac{\partial}{\partial \sigma_{t-1}} f^{\text{pca}}(\{\mathbf{U}_{i,t-1}\}_i, \mathbf{V}_{t-1}, \sigma_{t-1}) \right]^2
\end{aligned}$$

$$\begin{aligned}
& - \left(\frac{\eta_3}{2} - \frac{\eta_3^2 L_\sigma}{2} \right) \left[\frac{\partial}{\partial \sigma_{t-1}} f^{\text{pca}}(\{\mathbf{U}_{i,t-1}\}_i, \mathbf{V}_{t-1}, \sigma_{t-1}) \right]^2 \\
= & \frac{\eta_3}{2} \left[\left(\frac{1}{m} \sum_{i=1}^m \frac{\partial}{\partial \sigma_{t-1}} f_i^{\text{pca}}(\mathbf{U}_{i,t}, \mathbf{V}_t, \sigma_{t-1}) - \frac{\partial}{\partial \sigma_{t-1}} f_i^{\text{pca}}(\mathbf{U}_{i,t-1}, \mathbf{V}_t, \sigma_{t-1}) \right) \right. \\
& \left. + \frac{\partial}{\partial \sigma_{t-1}} f^{\text{pca}}(\{\mathbf{U}_{i,t-1}\}_i, \mathbf{V}_t, \sigma_{t-1}) - \frac{\partial}{\partial \sigma_{t-1}} f^{\text{pca}}(\{\mathbf{U}_{i,t-1}\}_i, \mathbf{V}_{t-1}, \sigma_{t-1}) \right]^2 \\
& - \left(\frac{\eta_3}{2} - \frac{\eta_3^2 L_\sigma}{2} \right) \left[\frac{\partial}{\partial \sigma_{t-1}} f^{\text{pca}}(\{\mathbf{U}_{i,t-1}\}_i, \mathbf{V}_{t-1}, \sigma_{t-1}) \right]^2 \\
\leq & \frac{\eta_3}{2} \left[\left(\frac{1}{m} \sum_{i=1}^m L_U^{(\sigma)} \|\mathbf{U}_{i,t} - \mathbf{U}_{i,t-1}\|_F \right) + L_V^{(\sigma)} \|\mathbf{V}_{i,t} - \mathbf{V}_{i,t-1}\|_F \right]^2 - \left(\frac{\eta_3 - \eta_3^2 L_\sigma}{2} \right) \left[\frac{\partial}{\partial \sigma_{t-1}} f^{\text{pca}}(\{\mathbf{U}_{i,t-1}\}_i, \mathbf{V}_{t-1}, \sigma_{t-1}) \right]^2 \\
& \hspace{15em} \text{(from Lemma 3.9)} \\
\leq & \frac{\eta_3}{2} \left[2 \left(\frac{1}{m} \sum_{i=1}^m L_U^{(\sigma)} \|\mathbf{U}_{i,t} - \mathbf{U}_{i,t-1}\|_F \right)^2 + 2 \left(L_V^{(\sigma)} \|\mathbf{V}_{i,t} - \mathbf{V}_{i,t-1}\|_F \right)^2 \right] - \left(\frac{\eta_3 - \eta_3^2 L_\sigma}{2} \right) \left[\frac{\partial}{\partial \sigma_{t-1}} f^{\text{pca}}(\{\mathbf{U}_{i,t-1}\}_i, \mathbf{V}_{t-1}, \sigma_{t-1}) \right]^2 \\
& \hspace{15em} \text{(since } (a+b)^2 \leq 2a^2 + 2b^2 \text{)} \\
\leq & \eta_3 \left[\frac{1}{m} \sum_{i=1}^m \left(L_U^{(\sigma)} \|\mathbf{U}_{i,t} - \mathbf{U}_{i,t-1}\|_F \right)^2 + \left(L_V^{(\sigma)} \|\mathbf{V}_{i,t} - \mathbf{V}_{i,t-1}\|_F \right)^2 \right] - \left(\frac{\eta_3 - \eta_3^2 L_\sigma}{2} \right) \left[\frac{\partial}{\partial \sigma_{t-1}} f^{\text{pca}}(\{\mathbf{U}_{i,t-1}\}_i, \mathbf{V}_{t-1}, \sigma_{t-1}) \right]^2 \\
& \hspace{15em} \text{(Cauchy-Schwarz inequality)} \\
= & \eta_3 (L_U^{(\sigma)})^2 \frac{1}{m} \left(\sum_{i=1}^m \|P_{\mathcal{T}_{\mathbf{U}_{i,t-1}}} (\nabla_{\mathbf{U}_{i,t-1}} f^{\text{pca}}(\mathbf{U}_{i,t-1}, \mathbf{V}_{t-1}, \sigma_{t-1}))\|_F^2 \right) + \eta_3 (L_V^{(\sigma)})^2 \|P_{\mathcal{T}_{\mathbf{V}_{t-1}}} (\nabla_{\mathbf{V}_{t-1}} f^{\text{pca}}(\{\mathbf{U}_{i,t}\}_i, \mathbf{V}_{t-1}, \sigma_{t-1}))\|_F^2 \\
& - \left(\frac{\eta_3 - \eta_3^2 L_\sigma}{2} \right) \left[\frac{\partial}{\partial \sigma_{t-1}} f^{\text{pca}}(\{\mathbf{U}_{i,t-1}\}_i, \mathbf{V}_{t-1}, \sigma_{t-1}) \right]^2.
\end{aligned}$$

Thus, we have

$$\begin{aligned}
& f^{\text{pca}}(\{\mathbf{U}_{i,t}\}_i, \mathbf{V}_t, \sigma_t) - f^{\text{pca}}(\{\mathbf{U}_{i,t-1}\}_i, \mathbf{V}_{t-1}, \sigma_{t-1}) \\
= & [f^{\text{pca}}(\{\mathbf{U}_{i,t}\}_i, \mathbf{V}_{t-1}, \sigma_{t-1}) - f^{\text{pca}}(\{\mathbf{U}_{i,t-1}\}_i, \mathbf{V}_{t-1}, \sigma_{t-1})] \\
& + [f^{\text{pca}}(\{\mathbf{U}_{i,t}\}_i, \mathbf{V}_t, \sigma_{t-1}) - f^{\text{pca}}(\{\mathbf{U}_{i,t}\}_i, \mathbf{V}_{t-1}, \sigma_{t-1})] \\
& + [f^{\text{pca}}(\{\mathbf{U}_{i,t}\}_i, \mathbf{V}_t, \sigma_t) - f^{\text{pca}}(\{\mathbf{U}_{i,t}\}_i, \mathbf{V}_t, \sigma_{t-1})] \\
\leq & \left(-\eta_1 + C\eta_1\eta_1^2 + \eta_3(L_U^{(\sigma)})^2 \right) \frac{1}{m} \sum_{i=1}^m \|P_{\mathcal{T}_{\mathbf{U}_{i,t-1}}} (\nabla_{\mathbf{U}_{i,t-1}} f_i^{\text{pca}}(\mathbf{U}_{i,t-1}, \mathbf{V}_{t-1}, \sigma_{t-1}))\|_F^2 \\
& + \left(-\eta_2 + C\eta_2\eta_2^2 + \eta_3(L_V^{(\sigma)})^2 \right) \|P_{\mathcal{T}_{\mathbf{V}_{t-1}}} (\nabla_{\mathbf{V}_{t-1}} f^{\text{pca}}(\{\mathbf{U}_{i,t}\}_i, \mathbf{V}_{t-1}, \sigma_{t-1}))\|_F^2 \\
& + \left(\frac{-\eta_3 + \eta_3^2 L_\sigma}{2} \right) \left[\frac{\partial}{\partial \sigma_{t-1}} f^{\text{pca}}(\{\mathbf{U}_{i,t-1}\}_i, \mathbf{V}_{t-1}, \sigma_{t-1}) \right]^2.
\end{aligned}$$

By choosing $\eta_1 = \min\{\frac{1}{3C\eta_1}, 1\}$, $\eta_2 = \min\{\frac{1}{3C\eta_2}, 1\}$, and $\eta_3 = \min\left\{\frac{\eta_1}{3(L_U^{(\sigma)})^2}, \frac{\eta_2}{3(L_V^{(\sigma)})^2}, \frac{1}{6L_\sigma}\right\}$, we have

$$\begin{aligned}
-\eta_1 + C\eta_1\eta_1^2 + \eta_3(L_U^{(\sigma)})^2 & \leq \eta_1 \left(C\eta_1\eta_1 - \frac{1}{3} \right) - \frac{2\eta_1}{3} + \frac{\eta_1}{3} = -\frac{\eta_1}{3}, \\
-\eta_2 + C\eta_2\eta_2^2 + \eta_3(L_V^{(\sigma)})^2 & \leq \eta_2 \left(C\eta_2\eta_2 - \frac{1}{3} \right) - \frac{2\eta_2}{3} + \frac{\eta_2}{3} = -\frac{\eta_2}{3}, \\
\frac{-\eta_3 + \eta_3^2 L_\sigma}{2} & = \eta_3 \left(L_\sigma\eta_3 - \frac{1}{6} \right) - \frac{\eta_3}{3} \leq -\frac{\eta_3}{3}.
\end{aligned}$$

Therefore, we obtain

$$\begin{aligned}
f^{\text{pca}}(\{\mathbf{U}_{i,t}\}_i, \mathbf{V}_t, \sigma_t) - f^{\text{pca}}(\{\mathbf{U}_{i,t-1}\}_i, \mathbf{V}_{t-1}, \sigma_{t-1}) &\leq -\frac{\eta_1}{3} \left(\frac{1}{m} \sum_{i=1}^m \|P_{\mathcal{T}_{\mathbf{U}_{i,t-1}}}(\nabla_{\mathbf{U}_{i,t-1}} f_i^{\text{pca}}(\mathbf{U}_{i,t-1}, \mathbf{V}_{t-1}, \sigma_{t-1}))\|_F^2 \right) \\
&\quad - \frac{\eta_2}{3} \|P_{\mathcal{T}_{\mathbf{V}_{t-1}}}(\nabla_{\mathbf{V}_{t-1}} f^{\text{pca}}(\{\mathbf{U}_{i,t}\}_i, \mathbf{V}_{t-1}, \sigma_{t-1}))\|_F^2 - \frac{\eta_3}{3} \left[\frac{\partial}{\partial \sigma_{t-1}} f^{\text{pca}}(\{\mathbf{U}_{i,t-1}\}_i, \mathbf{V}_{t-1}, \sigma_{t-1}) \right]^2.
\end{aligned}$$

□

A.1.7 Proof of Theorem 3.3

Proof. Following Lemma 3.10, by telescoping across the iterations, we have

$$\begin{aligned}
&\frac{1}{T} \sum_{t=1}^T \left[\|P_{\mathcal{T}_{\mathbf{V}_{t-1}}}(\nabla_{\mathbf{V}_{t-1}} f^{\text{pca}}(\{\mathbf{U}_{i,t}\}_i, \mathbf{V}_{t-1}, \sigma_{t-1}))\|_F^2 \right. \\
&\quad \left. + \left(\frac{1}{m} \sum_{i=1}^m \|P_{\mathcal{T}_{\mathbf{U}_{i,t-1}}}(\nabla_{\mathbf{U}_{i,t-1}} f_i^{\text{pca}}(\mathbf{U}_{i,t-1}, \mathbf{V}_{t-1}, \sigma_{t-1}))\|_F^2 \right) + \left[\frac{\partial}{\partial \sigma_{t-1}} f^{\text{pca}}(\{\mathbf{U}_{i,t-1}\}_i, \mathbf{V}_{t-1}, \sigma_{t-1}) \right]^2 \right] \\
&\leq \frac{1}{T \min\{\frac{\eta_1}{3}, \frac{\eta_2}{3}, \frac{\eta_3}{3}\}} \sum_{t=1}^T f^{\text{pca}}(\{\mathbf{U}_{i,t-1}\}_i, \mathbf{V}_{t-1}, \sigma_{t-1}) - f^{\text{pca}}(\{\mathbf{U}_{i,t}\}_i, \mathbf{V}_t, \sigma_t) \\
&= \frac{3(f^{\text{pca}}(\{\mathbf{U}_{i,0}\}_i, \mathbf{V}_0, \sigma_0) - f^{\text{pca}}(\{\mathbf{U}_{i,T}\}_i, \mathbf{V}_T, \sigma_T))}{T \min\{\eta_1, \eta_2, \eta_3\}}.
\end{aligned}$$

□

B Proofs for Adaptive AEs: ADEPT-AE

B.1 Proofs

B.1.1 Proof of Lemma 3.15

Proof. Following the same proof in Lemma 3.2, we have the same lower bound on σ_t if we initialized it in the same way.

The gradient w.r.t. $\boldsymbol{\mu}$ is

$$\nabla_{\boldsymbol{\mu}} f_i^{\text{ae}}(\boldsymbol{\theta}, \boldsymbol{\mu}, \sigma) = \frac{\boldsymbol{\mu} - \boldsymbol{\theta}}{2\sigma^2}.$$

Thus, we have

$$\left\| \frac{\boldsymbol{\mu}_1 - \boldsymbol{\theta}}{2\sigma^2} - \frac{\boldsymbol{\mu}_2 - \boldsymbol{\theta}}{2\sigma^2} \right\| = \left\| \frac{\boldsymbol{\mu}_1 - \boldsymbol{\mu}_2}{2\sigma^2} \right\| \leq \frac{d_\theta}{2\xi\omega^2} \|\boldsymbol{\mu}_1 - \boldsymbol{\mu}_2\| \leq L_\mu \|\boldsymbol{\mu}_1 - \boldsymbol{\mu}_2\|.$$

For L_σ , we have

$$\begin{aligned}
\left| \frac{\partial^2}{\partial \sigma^2} f_i^{\text{ae}}(\boldsymbol{\theta}, \boldsymbol{\mu}, \sigma) \right| &= \left| \frac{6\xi + 3\|\boldsymbol{\mu} - \boldsymbol{\theta}\|^2}{\sigma^4} - \frac{d_\theta}{\sigma^2} \right| \\
&\leq \left| \frac{6\xi + 3\|\boldsymbol{\mu} - \boldsymbol{\theta}\|^2}{\sigma^4} \right| + \left| \frac{d_\theta}{\sigma^2} \right| \\
&\leq \frac{6\xi + 3(2B)^2}{4\xi^2\omega^4/d_\theta^2} + \frac{d_\theta^2}{2\xi\omega^2} \\
&= \frac{3\xi d_\theta^2}{2\xi^2\omega^4} + \frac{3d_\theta^2 B^2}{\xi^2\omega^4} + \frac{d_\theta^2}{2\xi\omega^2} \\
&= L_\sigma.
\end{aligned}$$

For $L_\sigma^{(\mu)}$, we have

$$\begin{aligned}
\|\nabla_{\boldsymbol{\mu}} f_i^{\text{ae}}(\boldsymbol{\theta}, \boldsymbol{\mu}, \sigma_1) - \nabla_{\boldsymbol{\mu}} f_i^{\text{ae}}(\boldsymbol{\theta}, \boldsymbol{\mu}, \sigma_2)\| &= \left\| \frac{\boldsymbol{\mu} - \boldsymbol{\theta}}{2\sigma_1^2} - \frac{\boldsymbol{\mu} - \boldsymbol{\theta}}{2\sigma_2^2} \right\| \\
&= \left| \frac{1}{\sigma_1^2} - \frac{1}{\sigma_2^2} \right| \frac{\|\boldsymbol{\mu} - \boldsymbol{\theta}\|}{2} \\
&= |\sigma_1 - \sigma_2| \left| \frac{1}{\sigma_1^2\sigma_2} + \frac{1}{\sigma_1\sigma_2^2} \right| \frac{\|\boldsymbol{\mu} - \boldsymbol{\theta}\|}{2} \\
&\leq 2 \left(\omega \sqrt{\frac{2\xi}{d_\theta}} \right)^{-3} B |\sigma_1 - \sigma_2| \\
&= \frac{B \sqrt{d_\theta^3}}{\omega^3 \sqrt{2\xi^3}} |\sigma_1 - \sigma_2| \\
&= L_\sigma^{(\mu)} |\sigma_1 - \sigma_2|.
\end{aligned}$$

□

B.1.2 Proof of Theorem 3.12

Proof. Since $\boldsymbol{\mu}_t$ and σ_t are updated only when τ divides t , we consider the two cases separately.

When τ divides t First, for the sufficient decrease of $\boldsymbol{\theta}_{t,i}$, we have

$$\begin{aligned}
&f_i^{\text{ae}}(\boldsymbol{\theta}_{i,t}, \boldsymbol{\mu}_{t-1}, \sigma_{t-1}) - f_i^{\text{ae}}(\boldsymbol{\theta}_{i,t-1}, \boldsymbol{\mu}_{t-1}, \sigma_{t-1}) \\
&\leq \langle \nabla_{\boldsymbol{\theta}_{i,t-1}} f_i^{\text{ae}}(\boldsymbol{\theta}_{i,t-1}, \boldsymbol{\mu}_{t-1}, \sigma_{t-1}), \boldsymbol{\theta}_{i,t} - \boldsymbol{\theta}_{i,t-1} \rangle + \frac{L_\theta}{2} \|\boldsymbol{\theta}_{i,t} - \boldsymbol{\theta}_{i,t-1}\|^2 \\
&= \langle \nabla_{\boldsymbol{\theta}_{i,t-1}} f_i^{\text{ae}}(\boldsymbol{\theta}_{i,t-1}, \boldsymbol{\mu}_{t-1}, \sigma_{t-1}), -\eta_1 \nabla_{\boldsymbol{\theta}_{i,t-1}} f_i^{\text{ae}}(\boldsymbol{\theta}_{i,t-1}, \boldsymbol{\mu}_{t-1}, \sigma_{t-1}) \rangle + \frac{L_\theta}{2} \left\| -\eta_1 \nabla_{\boldsymbol{\theta}_{i,t-1}} f_i^{\text{ae}}(\boldsymbol{\theta}_{i,t-1}, \boldsymbol{\mu}_{t-1}, \sigma_{t-1}) \right\|^2 \\
&\leq \left(-\eta_1 + \eta_1^2 \frac{L_\theta}{2} \right) \left\| \nabla_{\boldsymbol{\theta}_{i,t-1}} f_i^{\text{ae}}(\boldsymbol{\theta}_{i,t-1}, \boldsymbol{\mu}_{t-1}, \sigma_{t-1}) \right\|^2.
\end{aligned}$$

Sum over the clients and we have

$$f^{\text{ae}}(\{\boldsymbol{\theta}_{i,t}\}, \boldsymbol{\mu}_{t-1}, \sigma_{t-1}) - f^{\text{ae}}(\{\boldsymbol{\theta}_{i,t-1}\}, \boldsymbol{\mu}_{t-1}, \sigma_{t-1}) \leq \left(-\eta_1 + \eta_1^2 \frac{L_\theta}{2} \right) \left(\frac{1}{m} \sum_{i=1}^m \left\| \nabla_{\boldsymbol{\theta}_{i,t-1}} f_i^{\text{ae}}(\boldsymbol{\theta}_{i,t-1}, \boldsymbol{\mu}_{t-1}, \sigma_{t-1}) \right\|^2 \right). \quad (18)$$

Second, for the sufficient decrease of σ_t , define

$$g_t^\sigma = \frac{1}{m} \sum_{i=1}^m \frac{\partial}{\partial \sigma_{t-1}} f_i^{\text{ae}}(\boldsymbol{\theta}_{i,t}, \boldsymbol{\mu}_{t-1}, \sigma_{t-1}).$$

Thus, $\sigma_t = \sigma_{t-1} - \eta_2 g_t^\sigma$ and

$$\begin{aligned}
f_i^{\text{ae}}(\boldsymbol{\theta}_{i,t}, \boldsymbol{\mu}_{t-1}, \sigma_t) - f_i^{\text{ae}}(\boldsymbol{\theta}_{i,t}, \boldsymbol{\mu}_{t-1}, \sigma_{t-1}) &\leq \left(\frac{\partial}{\partial \sigma_{t-1}} f_i^{\text{ae}}(\boldsymbol{\theta}_{i,t}, \boldsymbol{\mu}_{t-1}, \sigma_{t-1}) \right) (\sigma_t - \sigma_{t-1}) + \frac{L_\sigma}{2} (\sigma_t - \sigma_{t-1})^2 \\
&= \left(\frac{\partial}{\partial \sigma_{t-1}} f_i^{\text{ae}}(\boldsymbol{\theta}_{i,t}, \boldsymbol{\mu}_{t-1}, \sigma_{t-1}) \right) (-\eta_2 g_t^\sigma) + \frac{L_\sigma}{2} (-\eta_2 g_t^\sigma)^2.
\end{aligned}$$

Sum over the clients and we have

$$f^{\text{ae}}(\{\boldsymbol{\theta}_{i,t}\}, \boldsymbol{\mu}_{t-1}, \sigma_t) - f^{\text{ae}}(\{\boldsymbol{\theta}_{i,t}\}, \boldsymbol{\mu}_{t-1}, \sigma_{t-1}) \leq -\eta_2 (g_t^\sigma)^2 + \eta_2^2 \frac{L_\sigma}{2} (g_t^\sigma)^2 = \left(-\eta_2 + \eta_2^2 \frac{L_\sigma}{2} \right) (g_t^\sigma)^2. \quad (19)$$

Then, for the sufficient decrease of $\boldsymbol{\mu}_t$, define

$$\begin{aligned}\mathbf{g}_{i,t}^\mu &= \nabla_{\boldsymbol{\mu}_{t-1}} f_i^{\text{ae}}(\boldsymbol{\theta}_{i,t}, \boldsymbol{\mu}_{t-1}, \sigma_{t-1}), & \mathbf{g}_t^\mu &= \frac{1}{m} \sum_{i=1}^m \mathbf{g}_{i,t}^\mu, \\ \tilde{\mathbf{g}}_{i,t}^\mu &= \nabla_{\boldsymbol{\mu}_{t-1}} f_i^{\text{ae}}(\boldsymbol{\theta}_{i,t}, \boldsymbol{\mu}_{t-1}, \sigma_t), & \tilde{\mathbf{g}}_t^\mu &= \frac{1}{m} \sum_{i=1}^m \tilde{\mathbf{g}}_{i,t}^\mu.\end{aligned}$$

We have

$$\begin{aligned}f^{\text{ae}}(\{\boldsymbol{\theta}_{i,t}\}, \boldsymbol{\mu}_t, \sigma_t) - f^{\text{ae}}(\{\boldsymbol{\theta}_{i,t}\}, \boldsymbol{\mu}_{t-1}, \sigma_t) &\leq \langle \tilde{\mathbf{g}}_t^\mu, \boldsymbol{\mu}_t - \boldsymbol{\mu}_{t-1} \rangle + \frac{L_\mu}{2} \|\boldsymbol{\mu}_t - \boldsymbol{\mu}_{t-1}\|^2 \\ &= -\eta_3 \langle \tilde{\mathbf{g}}_t^\mu - \mathbf{g}_t^\mu + \mathbf{g}_t^\mu, \mathbf{g}_t^\mu \rangle + \frac{L_\mu \eta_3^2}{2} \|\mathbf{g}_t^\mu\|^2 \\ &= \left(-\eta_3 + \frac{L_\mu \eta_3^2}{2} \right) \|\mathbf{g}_t^\mu\|^2 + \eta_3 \langle \mathbf{g}_t^\mu - \tilde{\mathbf{g}}_t^\mu, \mathbf{g}_t^\mu \rangle \\ &\leq \left(-\eta_3 + \frac{L_\mu \eta_3^2}{2} \right) \|\mathbf{g}_t^\mu\|^2 + \frac{\eta_3}{2} \|\mathbf{g}_t^\mu - \tilde{\mathbf{g}}_t^\mu\|^2 + \frac{\eta_3}{2} \|\mathbf{g}_t^\mu\|^2 \\ &\leq \left(-\frac{\eta_3}{2} + \frac{L_\mu \eta_3^2}{2} \right) \|\mathbf{g}_t^\mu\|^2 + \frac{\eta_3 L_\sigma^{(\mu)^2}}{2} (\sigma_t - \sigma_{t-1})^2 \\ &\leq \left(-\frac{\eta_3}{2} + \frac{L_\mu \eta_3^2}{2} \right) \|\mathbf{g}_t^\mu\|^2 + \frac{\eta_3 \eta_2^2 L_\sigma^{(\mu)^2}}{2} (g_t^\sigma)^2 \\ &\leq \left(-\frac{\eta_3}{2} + \frac{L_\mu \eta_3^2}{2} \right) \|\mathbf{g}_t^\mu\|^2 + \frac{\eta_2^2 L_\sigma^{(\mu)^2}}{2} (g_t^\sigma)^2.\end{aligned}\tag{20}$$

Finally, we have the overall decrease when τ divides t by summing equation (19), (18), and (20),

$$\begin{aligned}f^{\text{ae}}(\{\boldsymbol{\theta}_{i,t}\}, \boldsymbol{\mu}_t, \sigma_t) - f^{\text{ae}}(\{\boldsymbol{\theta}_{i,t}\}, \boldsymbol{\mu}_{t-1}, \sigma_{t-1}) &\leq \left(-\eta_1 + \eta_1^2 \frac{L_\theta}{2} \right) \left(\frac{1}{m} \sum_{i=1}^m \|\nabla_{\boldsymbol{\theta}_{i,t-1}} f_i^{\text{ae}}(\boldsymbol{\theta}_{i,t-1}, \boldsymbol{\mu}_{t-1}, \sigma_{t-1})\|^2 \right) \\ &\quad + \left(-\eta_2 + \eta_2^2 \frac{L_\sigma + L_\sigma^{(\mu)^2}}{2} \right) (g_t^\sigma)^2 + \left(-\frac{\eta_3}{2} + \frac{L_\mu \eta_3^2}{2} \right) \|\mathbf{g}_t^\mu\|^2.\end{aligned}$$

When τ does not divide t At time steps that are not communication rounds we simply have decrease due to the updates of $\{\boldsymbol{\theta}_i\}$, that is,

$$\begin{aligned}f^{\text{ae}}(\{\boldsymbol{\theta}_{i,t}\}, \boldsymbol{\mu}_t, \sigma_t) - f^{\text{ae}}(\{\boldsymbol{\theta}_{i,t-1}\}, \boldsymbol{\mu}_{t-1}, \sigma_{t-1}) &= f^{\text{ae}}(\{\boldsymbol{\theta}_{i,t}\}, \boldsymbol{\mu}_{t-1}, \sigma_{t-1}) - f^{\text{ae}}(\{\boldsymbol{\theta}_{i,t-1}\}, \boldsymbol{\mu}_{t-1}, \sigma_{t-1}) \\ &= \frac{1}{m} \sum_{i=1}^m (f_i^{\text{ae}}(\boldsymbol{\theta}_{i,t}, \boldsymbol{\mu}_{t-1}, \sigma_{t-1}) - f_i^{\text{ae}}(\boldsymbol{\theta}_{i,t-1}, \boldsymbol{\mu}_{t-1}, \sigma_{t-1})) \\ &\leq \left(-\eta_1 + \eta_1^2 \frac{L_\theta}{2} \right) \left(\frac{1}{m} \sum_{i=1}^m \|\nabla_{\boldsymbol{\theta}_{i,t-1}} f_i^{\text{ae}}(\boldsymbol{\theta}_{i,t-1}, \boldsymbol{\mu}_{t-1}, \sigma_{t-1})\|^2 \right).\end{aligned}$$

The final bound By choosing, $\eta_1 = \frac{1}{L_\theta}$, $\eta_2 = \frac{1}{L_\sigma + L_\sigma^{(\mu)^2}}$, $\eta_3 = \min\{1, \frac{1}{L_\mu}\}$, and by averaging over time steps while combining two type of decrease, we obtain

$$\frac{1}{T} \sum_{t=1}^T \left(\frac{1}{m} \sum_{i=1}^m \|\nabla_{\boldsymbol{\theta}_{i,t-1}} f_i^{\text{ae}}(\boldsymbol{\theta}_{i,t-1}, \boldsymbol{\mu}_{t-1}, \sigma_{t-1})\|^2 \right) + \frac{1}{T} \sum_{\substack{t=1 \\ t\% \tau = 0}}^T \|\mathbf{g}_t^\mu\|^2 + \frac{1}{T} \sum_{\substack{t=1 \\ t\% \tau = 0}}^T (g_t^\sigma)^2 \leq \frac{\max\{L_\theta, L_\sigma + L_\sigma^{(\mu)^2}, L_\mu, 1\} \Delta_T}{T},$$

where $\Delta_T = f^{\text{ae}}(\{\boldsymbol{\theta}_{i,0}\}, \boldsymbol{\mu}_0, \sigma_0) - f^{\text{ae}}(\{\boldsymbol{\theta}_{i,T}\}, \boldsymbol{\mu}_T, \sigma_T)$. Given that τ is a finite constant let us denote $R = T/\tau$ as the number of communication rounds. Then we have,

$$\begin{aligned}
& \frac{1}{T} \sum_{t=1}^T \left(\frac{1}{m} \sum_{i=1}^m \|\mathbf{g}_{i,t}^\theta\|^2 \right) + \frac{1}{T} \sum_{\substack{t=1 \\ t\% \tau = 0}}^T \|\mathbf{g}_t^\mu\|^2 + \frac{1}{T} \sum_{\substack{t=1 \\ t\% \tau = 0}}^T (g_t^\sigma)^2 \\
&= \frac{R}{T} \left(\frac{1}{R} \sum_{t=1}^T \left(\frac{1}{m} \sum_{i=1}^m \|\mathbf{g}_{i,t}^\theta\|^2 \right) + \frac{1}{R} \sum_{\substack{t=1 \\ t\% \tau = 0}}^T \|\mathbf{g}_t^\mu\|^2 + \frac{1}{R} \sum_{\substack{t=1 \\ t\% \tau = 0}}^T (g_t^\sigma)^2 \right) \\
&\geq \frac{R}{T} \left(\frac{1}{R} \sum_{\substack{t=1 \\ t\% \tau = 0}}^T \left(\frac{1}{m} \sum_{i=1}^m \|\mathbf{g}_{i,t}^\theta\|^2 \right) + \frac{1}{R} \sum_{\substack{t=1 \\ t\% \tau = 0}}^T \|\mathbf{g}_t^\mu\|^2 + \frac{1}{R} \sum_{\substack{t=1 \\ t\% \tau = 0}}^T (g_t^\sigma)^2 \right) \\
&\geq \frac{R}{T} \min_{t \in [T], \tau | t} \left\{ \|\mathbf{g}_{i,t}^\theta\|^2 + \|\mathbf{g}_t^\mu\|^2 + (g_t^\sigma)^2 \right\}.
\end{aligned}$$

Finally this yields,

$$\min_{t \in [T], \tau | t} \left\{ \|\mathbf{g}_{i,t}^\theta\|^2 + \|\mathbf{g}_t^\mu\|^2 + (g_t^\sigma)^2 \right\} \leq \frac{\max\{L_\theta, L_\sigma + L_\sigma^{(\mu)^2}, L_\mu, 1\} \Delta_T^{\text{ae}}}{R},$$

where $\Delta_T^{\text{ae}} = f^{\text{ae}}(\{\boldsymbol{\theta}_{i,0}\}_i, \boldsymbol{\mu}_0, \sigma_0) - f^{\text{ae}}(\{\boldsymbol{\theta}_{i,T}\}_i, \boldsymbol{\mu}_T, \sigma_T)$.

□